High-frequency effective dynamical parameters for a viscoelastic layered medium modeling soft tissue

L. Flores-Cano and J. Bravo-Castillero

Unidad Académica Yucatán, Instituto de Investigaciones en Matemáticas Aplicadas y en Sistemas, Universidad Nacional Autónoma de Mexico, Tablaje Catastral N°6998, Mérida, 97357, Yucatán, Mexico.

L. D. Pérez-Fernández

Departamento de Matemática e Estatística, Instituto de Física e Matemática, Universidade Federal de Pelotas, Campus Universitário Capão do Leão, Caixa Postal 354, Pelotas, CEP 96010-971, Rio Grande do Sul, Brazil.

H. D. Sánchez-Chávez

Departamento de Física, Universidad Tecnológica de la Mixteca, Km. 2.5 Carretera a Acatlima, Huajuapan de León, Oaxaca, 69000, México.

Received 24 January 2026; accepted 17 April 2026

Shear wave propagation in a layered medium made of Voigt viscoelastic layers is studied. It is argued that it is possible to obtain closed-form analytical approximate expressions for the effective dynamical parameters of the layered medium in the high-frequency regime. The multiple-scale method is applied to obtain the frequency-dependent effective dynamical parameters. Lower-order analytical solution approximations for harmonic steady-state were obtained. Numerical comparison against precise numerical solutions via the transfer matrix method was carried out. This could contribute to the model design of tissue-like phantom materials for ultrasound devices calibration as well as in the processing of signals from shear wave elastography.

Keywords: Multiple scales; effective parameters; shear wave elastography; high-frecuency ultrasound.

DOI: https://doi.org/10.31349/RevMexFis.72.051101

1. Introduction

Ultrasound devices play an important role in present-day medical practice and research. The correct functioning of such devices depends, on the one hand, on the manufacturer and, on the other hand, on the final users (medical and technical staffs), the maintenance staff and the conditions of each device. When it comes to maintenance, it is necessary that the device be properly calibrated (several calibration techniques are summarized in Refs. [1,2]). Some calibration techniques are based on the use of phantoms, which mainly consist of a contact or propagation medium that is required to have dynamical parameters similar to those of the soft tissue to be analyzed, such as the average speed of sound, the acoustic impedance and the attenuation parameter (for the relevance of these quantities in the design of materials with specific dynamical parameters, see [3]). These parameters can be approximated using various materials and configurations. Typical materials include agar, gelatin and polyvinyl-alcohol solutions [4], whereas common configurations are cubes with embedded spheres or rods [5-7]. New phantom designs are frequently produced and evaluated [8-10]. In addition to practical experimental intuition, development of new phantoms can be guided by theoretical models based on the particularities of employed materials and configurations [11-14]. For instance, mathematical models would contribute not only to the rapid evaluation of these materials, but also to their design based on their geometry and frequency response. Therefore, understanding the propagation mechanisms in these materials would further the development of better design tools, which is the general objective of the present work. In particular, this contribution focuses on the mathematical modeling of the waves produced by medical ultrasound imaging devices. Such devices are considered here in the simplest conceptual form, that is, capable of producing ultrasonic waves through soft tissues and collecting the corresponding dispersion response signals for later processing [16,15].

We want to model soft tissue as simply as possible that lets us arrive at explicit parameter expressions as functions of frequency in the case of shear wave propagation. Speed propagation and attenuation of the wave are the goal parameters, whose expresions are expected to be of help as theoretical guide in some phantom design process. Soft tissue is an extremely complex medium composed by enormous number of diverse elements. Generally speaking, most models in literature assumed it to be a type of solid or fluid in which infinitesimal or finite, elastic or plastic strain relations govern [17-22]. Geometry composition is a major aspect here. Particularly a laminated model will be employed because of both its simplicity and resemblance to the structure of skin, as it is composed of layers of different tissues (epithelium, membranes, parenchyma thickness, etc.). In fact, the use of layered structural designs is recurrent to achieve specific functional parameters of materials for technological application, as a phantom propagation medium itself could be (see [23-27] among many others).

Each layer will be considered as a solid viscoelastic material [28], with Voigt constitutive relation. The simplicity and linearity of the Voigt constitutive relation are the first attributes that were considered for choosing it. Both Maxwell and Voigt models are very useful for simply modeling the viscosity of a medium (a good review can be seen in Ref. [29]). In particular, a good summary of the most common models of tissue mechanics and their limitations can be found in Ref. [30]. Particularly for the case of skin you can also consult [31]. Some authors have already pointed out that the best description of soft biological tissues is achieved with Voigt constitutive relation or some variation of this under the appropriate frequency ranges. Among the works in this regard you can see [32,33] where tissue substitute materials are treated.

To deal forward with the complexity of tissue layers we will take advantage from multiple scales homogenization method to obtain effective parameters [34,35] representing global behavior. The notion of effective parameter guiding us here is an abstract concept based on the black box model as follows: given two systems, S_1 and S_2, subject to the same boundary conditions, if the values of the response variables observed for system S_2 are sufficiently close to those obtained for system S_1, then system S_2 can be considered to be equivalent to (or a substitute for) system S_1. Thus, if the tissue substitute is a homogeneous material, then the constant parameters characterizing it are the so-called effective parameters of the substituted real tissue. Note that such a definition of effectiveness is pragmatic in nature [36], which differs from the ones based on the asymptotic homogenization methods [35] or averaging methods [37,38].

Section 2 presents the original continuum mechanics model of one-dimensional shear wave propagation in a non-homogeneous medium. Then, Sec. 3 states the perturbative model to be solved derived from the original one. Section 4 displays the solution process in detail to get the effective parameters. In Sec. 5 the approximated solution to the perturbative problem (based on effective parameters) and numerical solution to the original problem with transfer matrix method are compared for non-homogeneous media taken as random laminated ones.

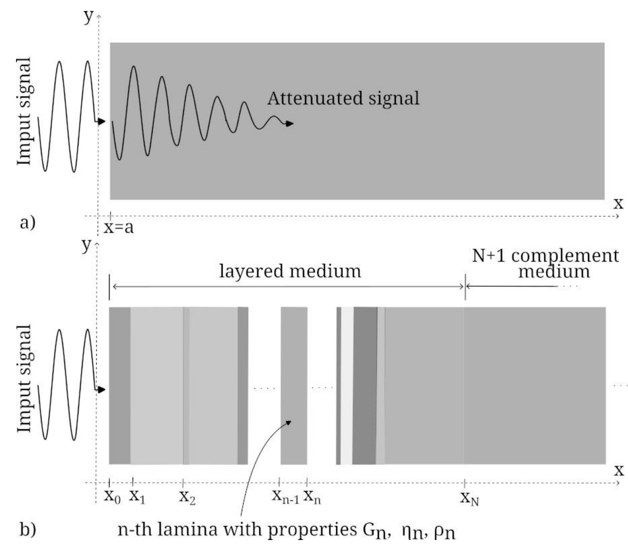

FIGURE 1. a) An imposed or entering signal and the corresponding propagated signal through a viscoelastic medium. b) Composite of N lamina, where x_n is the position of interfaces. The left boundary is at $x = x_0 = a$ and the right one is at $x = x_N$. In addition the wave is attenuated as $x \to \infty$.

2. The model

The linear problem to be treated is as follows:

$$\begin{cases} \hat{\rho}\dfrac{\partial^2 u}{\partial t^2} = \dfrac{\partial}{\partial x}\left(\hat{G}\dfrac{\partial u}{\partial x} + \hat{\eta}\dfrac{\partial^2 u}{\partial t \partial x}\right), \quad a \le x,\ 0 \le t, \\ u|_{x=a} = u_a \cos(\omega t), \\ \sigma|_{x=a} = \sigma_a \cos(\omega t + \theta_a). \end{cases} \tag{1}$$

Function $u(x,t)$ represents the displacement field of a transversal wave motion on a semi-infinite medium that extends over $[a,\infty) \ni x$ as shown in Fig. 1a). Constant parameters u_a, σ_a, θ_a and ω mean displacement amplitude, shear stress, response phase delay and harmonic frequency, respectively. Physically, the problem can be associated with a transversal plane wave induced in a pure normal way on the boundary $x = a$ of the medium. In addition, the medium is assumed to be layered [Fig. 1b)] as such non-homogeneity resembles many biological tissues. This continuum mechanical linear model is obtained from approximate Euler's motion equation $\partial_x \sigma = \rho \partial_{tt} u$ and Voigt's model $\sigma = \hat{G}\varepsilon + \hat{\eta}\partial_t \varepsilon$, where σ is the stress and $\varepsilon = \partial_x u$ is the strain. Parameters $\hat{G}$, $\hat{\eta}$ and $\hat{\rho}$ are the shear modulus, dynamical viscosity and density, respectively, that in general depends on x for a non-homogeneous medium. By the third Newton's law we expect that translational force density $\hat{\rho}\partial_{tt}u$ must be continuous throughout the whole domain in position x and time t, so the smoothness of u must be at least C^2 in t and C^0 in x, which implies that stress $\sigma = \hat{G}\partial_x u + \hat{\eta}\partial_{tx}u$ is at least C^1 in x, which means that $\hat{G}\partial_x u + \hat{\eta}\partial_{tx}u$ is C^1 but not necessarily each term and factor by itself. From the same Newton's law the deformative stress must be continuous too in x and t, so σ must be continuous. Thus, in case $\hat{G}$, $\hat{\eta}$ or $\hat{\rho}$ are piecewise continuous, these conditions must be satisfied in each boundary. On the other hand, there is a third condition that states the signal attenuation as it propagates to the right along the x-axis (which is a consequence of viscosity of the medium), *i.e.*

$$\lim_{x\to\infty} u(x,t) = 0, \tag{2}$$

which has the effect of relating the two boundary conditions.

A problem more suitable for computation associated with problem (1) can be stated in terms of complex functions as

$$\begin{cases} \dfrac{d}{dx}\left(G^*\dfrac{d\hat{w}}{dx}\right)+\omega^2\hat{\rho}\hat{w}=0, \quad a\leq x, \\ \hat{w}|_{x=a}=\hat{w}_a, \\ G^*\dfrac{d\hat{w}}{dx}\Big|_{x=a}=\hat{s}_a. \end{cases} \tag{3}$$

Problem (3) is obtained by changing to a problem where u is the real part of a complex function $W=u+\mathtt{i}v$ with v its imaginary part and supposing $W=\hat{w}(x)\exp(-\mathtt{i}\omega t)$ with function $\hat{w}$ carrying the spatial dependency. $\hat{w}_a$ and $\hat{s}_a$ are the corresponding boundary values of complex displacement $\hat{w}$ and complex stress $\hat{s}=G^*(d\hat{w}/dx)$ at $x=a$. $G^*(x,\omega)=\hat{G}(x)-\mathtt{i}\omega\hat{\eta}(x)$ is the so-called complex or dynamical modulus. Also, note that the parametric description in terms of frequency ω (instead of wave number) is adopted for attaining spatial attenuation rather than a temporal one [39].

Given Boltzmann's superposition principle for the constitutive relation of a viscoelastic material, $\sigma(x,t)=\int_0^t G(x,t-t')\partial_{t'}\varepsilon(x,t')$ considering no σ and ε for $t<0$ [29], its form in the frequency domain is $\sigma(x,\omega)=G^*(x,\omega)\varepsilon(x,\omega)$, where the function $G^*(x,\omega)$ is recognized as the complex modulus in its most general form. The material's properties are encapsulated in $G^*(x,\omega)$, so its behavior can be capricious, although subject to specific qualitative conditions at frequency limits close to zero or tending to infinity [40]. In a neighborhood of a frequency ω_0, a linear approximation $G^*(x,\omega)\approx G^*(x,\omega_0)+\partial_\omega G^*(x,\omega_0)(\omega-\omega_0)$ can be useful, which would have the form derived from Voigt model $G^*(x,\omega)\approx\hat{G}(x)-\mathtt{i}\hat{\eta}(x)\omega$. It is in this sense that the Voigt model will be used, where the determination of the values of $\hat{G}$ and $\hat{\eta}$ is done experimentally in the frequency range to be treated.

3. Perturbative problem

The multiple scales method is applied here to problem (3) in order to find an asymptotic approximation of its solution. The multiple scales method is a perturbation method that considers a formal power series expansion of the solution of a problem depending on a small parameter [34,41]. The method requires, in addition to the expansion parameter, the definition of two or more hierarchical scale variables which in this case are space variables ranked according to the powers of the expansion parameter.

3.1. Dimensionless formulation

We want to explore the asymptotic behavior in the high-frequency regime. On the other hand, higher frequency implies shorter wavelength, so the microstructural details of the propagation medium of characteristic length smaller than this wavelength remain undetected by the wave, as they appear as homogeneous regions at its resolution scale. Then, the wavelength is taken as the scale of observation, that is, the unit length from which the medium is seen as a nested hierarchy of homogeneous blocks that extend longitudinally in powers of such a unit. In particular, if the medium is overdamped, the wave attenuates before propagating more than one wavelength so, in this case, the mean attenuation length can also serve as an observation scale.

An appropriate choice of the small expansion parameter allows, in addition to a good approximation, simplification in solving the problem. We are interested in exploring the frequency domain as $\omega\to+\infty$, hence a small parameter inverse to the frequency makes sense. The following dimensionless variables are proposed: $x=l\xi$, $w(\xi)=\hat{w}(l\xi)/l$, $\xi_a=a/l$, $w_a=\hat{w}_a/l$, $G(\xi)=\hat{G}(l\xi)/\tilde{G}$, $\eta(\xi)=\hat{\eta}(l\xi)/\tilde{\eta}$, $\rho(\xi)=\hat{\rho}(l\xi)/\tilde{\rho}$, $s_a=\hat{s}_a/\omega\tilde{\eta}$, $\epsilon=\tilde{G}/(\omega\tilde{\eta})$ y $l=\sqrt{\tilde{G}/(\omega^2\tilde{\rho})}$, with which problem (3) becomes

$$\begin{cases} \dfrac{d}{d\xi}\left((\epsilon G-\mathtt{i}\eta)\dfrac{dw}{d\xi}\right)+\epsilon\rho w=0, \quad \xi_a\leq\xi, \\ w(\xi)|_{\xi=\xi_a}=w_a, \\ (\epsilon G-\mathtt{i}\eta)\dfrac{dw}{d\xi}\Big|_{\xi=\xi_a}=s_a. \end{cases} \tag{4}$$

$\tilde{G}$, $\tilde{\eta}$ and $\tilde{\rho}$ are suitable constant values, for example, their corresponding maximum or mean values through the layered medium could work.

3.2. The expansion parameter

The value of parameter ϵ for tissue and ultrasonic scanning frequency is of order $\mathcal{O}(10^{-6})$, which is coherent with the fact that $\omega\hat{\eta}\gg\hat{G}$ for high frequency values, so ϵ is a good candidate for expansion parameter. As choosing adequate expansion parameter and parametrization strategy is crucial [42,43], it proves useful to take the expansion parameter $\nu=\sqrt{\epsilon}$ to avoid fractional powers of ϵ, although working with fractional power expansions is possible [44]. Thus, the problem to be solved is

$$\begin{cases} \dfrac{d}{d\xi}\left((\nu^2 G-\mathtt{i}\eta)\dfrac{dw}{d\xi}\right)+\nu^2\rho w=0, \quad \xi_a\leq\xi, \\ w(\xi)|_{\xi=\xi_a}=w_a(\nu), \\ (\nu^2 G-\mathtt{i}\eta)\dfrac{dw}{d\xi}\Big|_{\xi=\xi_a}=s_a(\nu). \end{cases} \tag{5}$$

Following [45], the solution to problem (5) is sought via the asymptotic expansions

$$\begin{aligned}
w(\xi) &= w_0(\xi_0,\xi_1,\xi_2,\ldots) + \nu w_1(\xi_0,\xi_1,\xi_2,\ldots) + \nu^2 w_2(\xi_0,\xi_1,\xi_2,\ldots) + \ldots,\\
\frac{d}{d\xi} &= \frac{df_0}{d\xi}\frac{\partial}{\partial\xi_0} + \nu\frac{df_1}{d\xi}\frac{\partial}{\partial\xi_1} + \nu^2\frac{df_2}{d\xi}\frac{\partial}{\partial\xi_2} + \cdots\\
w_a &= w_{a0} + \nu w_{a1} + \nu^2 w_{a2} + \ldots,\\
s_a &= s_{a0} + \nu s_{a1} + \nu^2 s_{a2} + \ldots,
\end{aligned} \tag{6}$$

where $\xi_m = \nu^m f_m(\xi)$, $m = 0,1,2\ldots$, are the rescaling variables, f_m are functions to be determined, and ξ_0 is the reference or original variable, that is, $f_0(\xi) = \xi$ and therefore, $\xi_0 = \xi$, then $\xi_m = \nu^m f_m(\xi_0)$. So, variables ξ_m will be treated as independent of each other except for ξ_0. The w_m (with $m = 0,1,2,\ldots$) is the m-th coefficient of the formal series of w in powers of ν, and is expected behave asymptotically at least like w_{m-1} to ensure term $v^m w_m$ has a contribution of order $\mathcal{O}(\nu^m)$ to the solution w. Coefficients $f'_m d/d\xi_m$ of differential operator should be understood in the same way. Expansions for boundary values were propoused because it is expected they depend on frecuency, at the same time expansion parameter is expected to be related inversely with frecuency that is supposed to be high enough. So, coefficients w_{am} and s_{am} could be understood as expansion coefficients in the sense of Taylor's series.

By substituting (6) into the differential equation of problem (5), followed by some manipulations and grouping by powers of ν, the asymptotically zero expression is obtained which, to be satisfied, the coefficients powers of ν must be zero, that is,

$$\sum_{l+m+n=\tilde{n}} f'_l\frac{\partial}{\partial\xi_l}\left(\eta f'_m\frac{\partial w_n}{\partial\xi_m}\right) + \mathtt{i}\sum_{l+m+n=\tilde{n}-2} f'_l\frac{\partial}{\partial\xi_l}\left(G f'_m\frac{\partial w_n}{\partial\xi_m}\right) + \mathtt{i}\rho w_{\tilde{n}-2} = 0, \quad l,m,n,\tilde{n}\in\{0,1,2,\ldots\}. \tag{7}$$

The sum subject to condition $l+m+n=\tilde{n}$ means that if $\tilde{n}=0$ then $(l,m,n)=(0,0,0)$ and the sum has a single term; if $\tilde{n}=1$ then the sum has three terms for $(l,m,n)=(1,0,0)$, $(l,m,n)=(0,1,0)$ and $(l,m,n)=(0,0,1)$; and so on for $\tilde{n}\geq 2$. It is agreed that $f'_m=0$ and $w_m=0$ in case $m<0$. The boundary and attenuation conditions are also expanded, which yields

$$\begin{cases}
w_n|_{\xi=\xi_a} = w_{an},\\
s_{an} = \left.\left(G\displaystyle\sum_{l+m=n-2} f'_l\frac{\partial w_m}{\partial\xi_l} - \mathtt{i}\eta\sum_{l+m=n} f'_l\frac{\partial w_m}{\partial\xi_l}\right)\right|_{\xi=\xi_a},\\
\displaystyle\lim_{\xi\longrightarrow\infty} w_m = 0, \quad l,m,n\in\{0,1,2,\ldots\},
\end{cases} \tag{8}$$

where the rules just described for indices are the same here. The last condition is the already stated attenuation condition expected for each w_m.

4. Effective parameters

First, take $\tilde{n}=0$ in Eq. (7) and $n=0$ (8), so the zeroth-order problem is

$$\nu^0:\begin{cases}
f'_0\dfrac{\partial}{\partial\xi_0}\left(\eta f'_0\dfrac{\partial w_0}{\partial\xi_0}\right) = 0,\\
w_0|_{\xi=\xi_a} = w_{a0},\\
-\mathtt{i}\eta f'_0\left.\dfrac{\partial w_0}{\partial\xi_0}\right|_{\xi=\xi_a} = s_{a0},\\
\displaystyle\lim_{\xi_0\longrightarrow\infty} w_0 = 0.
\end{cases} \tag{9}$$

whose differential equation is easily integrated to obtain the general solution

$$\begin{aligned}
w_0 = A_0(\xi_1,\xi_2,\ldots)&\int_{\xi_a}^{\xi_0}\frac{1}{\eta(\mu)f'_0(\mu)}d\mu\\
&+ B_0(\xi_1,\xi_2,\ldots),
\end{aligned} \tag{10}$$

where A_0 and B_0 are the integration constants with respect to the integration variable ξ_0, and $f'_0\equiv 1$. Note that A_0 and B_0 do not depend explicitly on ξ_0 but through the other ξ_m ($m=1,2,\ldots$). However, expresion (10) doesn't met the attenuation condition in general for a $\eta(\xi)$ strictly positive function, for example, a piecewise constant function which is the case for layered medium has an integral would grows unboundedly when $\xi_0\rightarrow\infty$. As a consequence A_0 must be identically zero, implying too the zero first contribution to the response signal, $s_{a0}=0$. Thus, the information gathered from the zeroth-order problem is

$$\left.\begin{aligned}
-\mathtt{i}\ A_0|_{\xi=\xi_a} &= s_{a0},\\
B_0|_{\xi=\xi_a} &= w_{a0},\\
A_0 &= 0,\\
s_{a0} &= 0,\\
w_0 &= B_0(\xi_1,\xi_2,\ldots),\\
\frac{\partial w_0}{\partial\xi_0} &= 0.
\end{aligned}\right\}:\nu^0 \tag{11}$$

Now, take $\tilde{n} = 1$ in (7) and $n = 1$ in (8), so the first-order problem is

$$\nu^1 : \begin{cases} f_0' \dfrac{\partial}{\partial \xi_0}\left(\eta f_0' \dfrac{\partial w_1}{\partial \xi_0}\right) = -f_0' \dfrac{\partial}{\partial \xi_0}\left(\eta f_1' \dfrac{\partial w_0}{\partial \xi_1}\right) \\ \quad - f_1' \dfrac{\partial}{\partial \xi_1}\left(\eta f_0' \dfrac{\partial w_0}{\partial \xi_0}\right), \\ w_1|_{\xi=\xi_a} = w_{a1}, \\ -\mathtt{i}\eta \left(f_0' \dfrac{\partial w_1}{\partial \xi_0} + f_1' \dfrac{\partial w_0}{\partial \xi_1}\right)\Bigg|_{\xi=\xi_a} = s_{a1}, \\ \lim\limits_{\xi_0 \longrightarrow \infty} w_1 = 0, \end{cases} \tag{12}$$

where terms containing $\partial w_0/\partial \xi_0 = 0$ can be eliminated. Then, direct integration provides the general solution as

$$w_1 = -\frac{\partial B_0}{\partial \xi_1} \int \left\{\frac{f_1'}{f_0'}\right\} + A_1 \int \left\{\frac{1}{\eta f_0'}\right\} + B_1, \tag{13}$$

where the limits $\xi_a = a/l$ (lower), ξ_0 (upper) and the integration variable ξ_0 have been omitted for the sake of brevity and their respective integrads were embraced, which will be done from now on unless otherwise indicated. The dependencies of each variable were also omitted, A_1 and B_1 being the integration constants with respect to ξ_0. As before, A_1 and $\partial B_0/\partial \xi_1$ must be restricted to satisfy the attenuation condition. Lighthill anti-secularism criterion [46] in its relaxed form

$$\frac{w_{n+1}}{w_n} \sim \text{const.}, \forall \xi_m \to \infty, \quad m, n \in \{0, 1, 2, \ldots\}, \tag{14}$$

provides a way to proceed. Here, it means that the contribution w_1 behaves as w_0 as $\xi_0 \to \infty$. Since w_0 is constant with respect to ξ_0, then w_1 should also be constant at least in the limit. Then, the Lighthill criterion becomes

$$\begin{aligned} &-\frac{\partial B_0}{\partial \xi_1} \int \left\{\frac{f_1'}{f_0'}\right\} \\ &+ A_1 \int \left\{\frac{1}{\eta f_0'}\right\} \sim \text{const.}, \quad \text{as } \xi_0 \to \infty, \end{aligned} \tag{15}$$

The constant in the right-hand side of (15) is zero because the left-hand side expression is zero in $\xi_0 = \xi_a$ and, also, because the attenuation condition requires it. Then, we have

$$\lim_{\xi_0 \to \infty} \left(-\frac{\partial B_0}{\partial \xi_1} \int \left\{\frac{f_1'}{f_0'}\right\} + A_1 \int \left\{\frac{1}{\eta f_0'}\right\}\right) = 0,$$

$$\Longrightarrow \frac{A_1}{\frac{\partial B_0}{\partial \xi_1}} = \lim_{\xi_0 \to \infty} \frac{\int \left\{\frac{f_1'}{f_0'}\right\}}{\int \left\{\frac{1}{\eta f_0'}\right\}} = \text{const.}, \quad \frac{\partial B_0}{\partial \xi_1} \neq 0,$$

Hence, with constant α_{01},

$$A_1 = \alpha_{01} \frac{\partial B_0}{\partial \xi_1} \tag{16}$$

and, therefore,

$$\alpha_{01} = \lim_{\xi_0 \to \infty} \frac{\int \left\{\frac{f_1'}{f_0'}\right\}}{\int \left\{\frac{1}{\eta f_0'}\right\}}. \tag{17}$$

Condition (17) on f_1 indicates that this function must be $\mathcal{O}(\int \eta^{-1})$ provided there is a solution. This condition is similar to the one used in Ref. [47] in the discussion of the multiple scales method for homogenization.

By putting the definition

$$g_{01}(\xi_0) = \alpha_{01} \int \left\{\frac{1}{\eta f_0'}\right\} - \int \left\{\frac{f_1'}{f_0'}\right\}, \tag{18}$$

into (13) with (16), w_1 is written as $w_1 = g_{01} \partial B_0/\partial \xi_1 + B_1$. Such a consideration, together with (11) in the first-order problem (12), leads to $B_1|_{\xi=\xi_a} = w_{a1}$ and $-\mathtt{i}\alpha_{01}(\partial B_0/\partial \xi_1)|_{\xi=\xi_a} = s_{a1}$, so the first-order information is

$$\left.\begin{aligned} s_{a0} &= 0, \\ w_0 &= B_0(\xi_1, \xi_2, \ldots), \\ B_0|_{\xi=\xi_a} &= w_{a0}, \\ -\mathtt{i}\alpha_{01} \frac{\partial B_0}{\partial \xi_1}\bigg|_{\xi=\xi_a} &= s_{a1}, \\ w_1 &= g_{01}(\xi) \frac{\partial B_0}{\partial \xi_1}(\xi_1, \xi_2, \ldots) \\ &\quad + B_1(\xi_1, \xi_2, \ldots), \\ B_1|_{\xi=\xi_a} &= w_{a1}. \end{aligned}\right\} : \nu^1 \tag{19}$$

Next, take $\tilde{n} = 2$ in (7) and $n = 2$ in (8), so the second-order problem is

$$\nu^2 : \begin{cases} f_0' \dfrac{\partial}{\partial \xi_0}\left(\eta f_0' \dfrac{\partial w_2}{\partial \xi_0}\right) = -f_0' \dfrac{\partial}{\partial \xi_0}\left(\eta f_1' \dfrac{\partial w_1}{\partial \xi_1}\right) \\ \quad - f_1' \dfrac{\partial}{\partial \xi_1}\left(\eta f_0' \dfrac{\partial w_1}{\partial \xi_0}\right) - f_0' \dfrac{\partial}{\partial \xi_0}\left(\eta f_2' \dfrac{\partial w_0}{\partial \xi_2}\right) \\ \quad - f_1' \dfrac{\partial}{\partial \xi_1}\left(\eta f_1' \dfrac{\partial w_0}{\partial \xi_1}\right) - f_2' \dfrac{\partial}{\partial \xi_2}\left(\eta f_0' \dfrac{\partial w_0}{\partial \xi_0}\right) \\ \quad - \mathtt{i} f_0' \dfrac{\partial}{\partial \xi_0}\left(G f_0' \dfrac{\partial w_0}{\partial \xi_0}\right) - \mathtt{i}\rho w_0, \\ w_2|_{\xi=\xi_a} = w_{a2}, \\ s_{a2} = G f_0' \dfrac{\partial w_0}{\partial \xi_0}\bigg|_{\xi=\xi_a} \\ \quad -\mathtt{i}\eta \left(f_0' \dfrac{\partial w_2}{\partial \xi_0} + f_1' \dfrac{\partial w_1}{\partial \xi_1} + f_2' \dfrac{\partial w_0}{\partial \xi_2}\right)\Bigg|_{\xi=\xi_a}, \\ \lim\limits_{\xi_0 \longrightarrow \infty} w_2 = 0, \end{cases} \tag{20}$$

which, by using the information in (19), produces the general solution

$$
\begin{aligned}
w_2 = &-\left(\alpha_{01}\left(\int\left\{\frac{f_1'}{f_0'}\int\frac{1}{\eta f_0'}\right\}+\int\left\{\frac{1}{\eta f_0'}\int\frac{f_1'}{f_0'}\right\}\right)\right.\\
&\left.-\int\left\{\frac{f_1'}{f_0'}\int\frac{f_1'}{f_0'}\right\}\right)\frac{\partial^2 B_0}{\partial\xi_1^2}-\mathtt{i}\int\left\{\frac{1}{\eta f_0'}\int\frac{\rho}{f_0'}\right\}B_0\\
&-\int\left\{\frac{f_1'}{f_0'}\right\}\frac{\partial B_1}{\partial\xi_1}-\int\left\{\frac{f_2'}{f_0'}\right\}\frac{\partial B_0}{\partial\xi_2}+\int\left\{\frac{1}{\eta f_0'}\right\}A_2\\
&+B_2,
\end{aligned}
$$

where braces delimiting integrad of inner integrals were omitted because the scopes of these integrals are deduced from the outer ones. A_2 and B_2 are the integration constants that depend on ξ_n, $n>0$. In this case, the Lighthill criterion (14) involves all terms but B_2, since the same reasons given to eliminate first term of expresion (10) apply here too. Then, the criterion becomes

$$
\begin{aligned}
&-\left(\alpha_{01}\left(\int\left\{\frac{f_1'}{f_0'}\int\frac{1}{\eta f_0'}\right\}+\int\left\{\frac{1}{\eta f_0'}\int\frac{f_1'}{f_0'}\right\}\right)\right.\\
&\left.-\int\left\{\frac{f_1'}{f_0'}\int\frac{f_1'}{f_0'}\right\}\right)\frac{\partial^2 B_0}{\partial\xi_1^2}-\mathtt{i}\int\left\{\frac{1}{\eta f_0'}\int\frac{\rho}{f_0'}\right\}B_0\\
&-\int\left\{\frac{f_1'}{f_0'}\right\}\frac{\partial B_1}{\partial\xi_1}-\int\left\{\frac{f_2'}{f_0'}\right\}\frac{\partial B_0}{\partial\xi_2}+\int\left\{\frac{1}{\eta f_0'}\right\}A_2\\
&\sim \text{const.},\quad \text{as } \xi_0\longrightarrow\infty.
\end{aligned}
\tag{21}
$$

In this case, as we are looking for a wave-type solution, the terms of $\partial^2 B_0/\partial\xi_1^2$ and B_0 could form a wave equation, whereas, analogously to the previous first-order case, the remaining terms can be related to a suitable form of A_2. This approach is reinforced by the fact that the coefficients in these term association proposals are of the same integration order. So, it is more natural to establish a proportionality relation between, for example, the coefficients of $\partial B_1/\partial\xi_1$ and A_2 than between the coefficients of B_0 and $\partial B_0/\partial\xi_2$. Of course, one must keep in mind that f_1 behaves asymptotically as the first-order integral of η^{-1}, so its participation would count as an order of integration. With such considerations, criterion (21) is decomposed into two parts as

$$
\begin{aligned}
&-\left(\alpha_{01}\left(\int\left\{\frac{f_1'}{f_0'}\int\frac{1}{\eta f_0'}\right\}+\int\left\{\frac{1}{\eta f_0'}\int\frac{f_1'}{f_0'}\right\}\right)\right.\\
&\left.-\int\left\{\frac{f_1'}{f_0'}\int\frac{f_1'}{f_0'}\right\}\right)\frac{\partial^2 B_0}{\partial\xi_1^2}-\mathtt{i}\int\left\{\frac{1}{\eta f_0'}\int\frac{\rho}{f_0'}\right\}B_0\sim\text{const.},\\
&-\int\left\{\frac{f_1'}{f_0'}\right\}\frac{\partial B_1}{\partial\xi_1}-\int\left\{\frac{f_2'}{f_0'}\right\}\frac{\partial B_0}{\partial\xi_2}\\
&+\int\left\{\frac{1}{\eta f_0'}\right\}A_2\sim\text{const., as } \xi_0\longrightarrow\infty.
\end{aligned}
\tag{22}
$$

Now, reasoning as in the first-order case, we propose

$$
\begin{aligned}
\frac{\partial^2 B_0}{\partial\xi_1^2}&=-\kappa_{01}^2 B_0,\\
A_2&=\alpha_{11}\frac{\partial B_1}{\partial\xi_1}+\alpha_{02}\frac{\partial B_0}{\partial\xi_2},
\end{aligned}
\tag{23}
$$

from which the following conditions are obtained:

$$
\begin{aligned}
\lim_{\xi_0\to\infty}&\left(\left(\alpha_{01}\left(\int\left\{\frac{f_1'}{f_0'}\int\frac{1}{\eta f_0'}\right\}+\int\left\{\frac{1}{\eta f_0'}\int\frac{f_1'}{f_0'}\right\}\right)\right.\right.\\
&\left.\left.-\int\left\{\frac{f_1'}{f_0'}\int\frac{f_1'}{f_0'}\right\}\right)\kappa_{01}^2-\mathtt{i}\int\left\{\frac{1}{\eta f_0'}\int\frac{\rho}{f_0'}\right\}\right)=0,
\end{aligned}
\tag{24}
$$

$$
\lim_{\xi_0\to\infty}\left(\alpha_{11}\int\left\{\frac{1}{\eta f_0'}\right\}-\int\left\{\frac{f_1'}{f_0'}\right\}\right)=0, \tag{25}
$$

$$
\lim_{\xi_0\to\infty}\left(\alpha_{02}\int\left\{\frac{1}{\eta f_0'}\right\}-\int\left\{\frac{f_2'}{f_0'}\right\}\right)=0, \tag{26}
$$

where κ_{01}, α_{11} and α_{02} are suitable constants. Condition (25) for f_1 is the same as (17) provided that $\alpha_{11}=\alpha_{01}$, which is assumed to avoid contradiction. Also, condition (26) for f_2 is analogous to that for f_1 with its corresponding asymptotic proportionality constant α_{02}. As for condition (24), it can be reduced to see that it is indeed consistent with the proposals made, so κ_{01} can be obtained.

Consider the definition

$$
\begin{aligned}
g_2(\xi_0)=&\left(\alpha_{01}\left(\int\left\{\frac{f_1'}{f_0'}\int\frac{1}{\eta f_0'}\right\}+\int\left\{\frac{1}{\eta f_0'}\int\frac{f_1'}{f_0'}\right\}\right)\right.\\
&\left.-\int\left\{\frac{f_1'}{f_0'}\int\frac{f_1'}{f_0'}\right\}\right)\kappa_{01}^2-\mathtt{i}\int\left\{\frac{1}{\eta f_0'}\int\frac{\rho}{f_0'}\right\},
\end{aligned}
\tag{27}
$$

recall that $f_0'=1$, and impose $f_1(\xi_0)|_{\xi=\xi_a}=0$ since it is a perturbation to ξ_0 as [41]

$$
\begin{aligned}
\xi&\sim\xi_0+\xi_1+\xi_2+\cdots\\
&=\xi_0+\nu f_1(\xi_0)+\nu^2 f_2(\xi_0)+\cdots.
\end{aligned}
\tag{28}
$$

Then, (27) becomes

$$
\begin{aligned}
g_2(\xi_0)=&\frac{1}{2}f_1\left(\alpha_{01}\int\left\{\frac{1}{\eta}\right\}+\left(\alpha_{01}\int\left\{\frac{1}{\eta}\right\}-f_1\right)\right)\kappa_{01}^2\\
&-\mathtt{i}\int\left\{\frac{1}{\eta}\int\rho\right\},
\end{aligned}
$$

where expression inside inner parentheses is just (18), which tends to zero when $\xi_0\to\infty$ due to condition (17). Taking the limit $\xi_0\to\infty$ for (27) also becomes zero implying

$$
\kappa_{01}^2=2\mathtt{i}\lim_{\xi_0\to\infty}\frac{\int\left\{\frac{1}{\eta}\int\rho\right\}}{\left(\alpha_{01}\int\left\{\frac{1}{\eta}\right\}\right)^2}, \tag{29}
$$

Formula (29) is the definition of κ_{01} or, more precisely, its shape. At the same time, it is a condition on the parameters of the medium, that is, in order for κ_{01} to be finite, it is necessary that the second-order integral in the numerator grows asymptotically at the same rate as the square of the first-order integral in the denominator, which restricts the choice of parameters ρ and η. For instance, if we consider the case of a homogeneous medium (with constant parameters), both numerator and denominator are polynomials of degree two, so they have the same asymptotic behavior. Also, for a layered medium composed of homogeneous layers whose parameter values oscillate around their constant effective values, this assumption seems to be sensible as well.

By taking κ_{01} as the principal square root of (29), the general solution of (23) is $B_0 = C_0(\xi_2,\ldots)\exp(\mathtt{i}\kappa_{01}\xi_1(\xi_0)) + D_0(\xi_2,\ldots)\exp(-\mathtt{i}\kappa_{01}\xi_1(\xi_0))$, from which the contributions of right- and left-traveling waves are evident. By using the boundary conditions in (19), it follows that $C_0|_{\xi=\xi_a} = (\alpha_{01}\kappa_{01})^{-1}(\alpha_{01}\kappa_{01}w_{a0} + s_{a1})$ and $D_0|_{\xi=\xi_a} = (\alpha_{01}\kappa_{01})^{-1}(\alpha_{01}\kappa_{01}w_{a0} - s_{a1})$, where $\xi_1|_{\xi=\xi_a} = 0$ because $f_1|_{\xi=\xi_a} = 0$. As the real and imaginary parts of κ_{01} are positive, the second term diverges as $\xi_0 \to \infty$, so the attenuation condition implies $D_0 = 0$, leading to the first contribution to the response signal $s_{a1} = \alpha_{01}\kappa_{01}w_{a0}$, which produces $B_0 = C_0(\xi_2,\ldots)\exp(\mathtt{i}\kappa_{01}\xi_1(\xi_0))$ with $C_0|_{\xi=\xi_a} = w_{a0}$.

In order to know the behavior of w_0, it is still necessary to find f_1, which in turn requires the analysis of the following order ($\tilde{n} = 3$ in (7) and $n = 3$ in (8)). Define

$$g_{11}(\xi_0) = \alpha_{11}\int\left\{\frac{1}{\eta f_0'}\right\} - \int\left\{\frac{f_1'}{f_0'}\right\} \tag{30}$$

and

$$g_{02}(\xi_0) = \alpha_{02}\int\left\{\frac{1}{\eta f_0'}\right\} - \int\left\{\frac{f_2'}{f_0'}\right\}, \tag{31}$$

so the second-order information is

$$\left.\begin{aligned}
&B_0 = C_0(\xi_2,\ldots)\exp\left(\mathtt{i}\kappa_{01}\xi_1\left(\xi_0\right)\right),\\
&C_0|_{\xi=\xi_a} = w_{a0},\\
&w_0 = B_0,\\
&s_{a0} = 0,\\
&w_1 = \mathtt{i}\kappa_{01}g_{01}B_0 + B_1,\\
&B_1|_{\xi=\xi_a} = w_{a1},\\
&s_{a1} = \alpha_{01}\kappa_{01}w_{a0},\\
&w_2 = g_2B_0 + g_{11}\frac{\partial B_1}{\partial\xi_1} + g_{02}\frac{\partial B_0}{\partial\xi_2} + B_2,\\
&B_2|_{\xi=\xi_a} = w_{a2},\\
&-\mathtt{i}\left(\alpha_{11}\frac{\partial B_1}{\partial\xi_1} + \alpha_{02}\frac{\partial B_0}{\partial\xi_2}\right)\bigg|_{\xi=\xi_a} = s_{a2}.
\end{aligned}\right\} : \nu^2 \tag{32}$$

Next, take $\tilde{n} = 3$ in (7) and $n = 3$ in (8), so the third-order problem is

$$\nu^3 : \begin{cases}
f_0'\dfrac{\partial}{\partial\xi_0}\left(\eta f_0'\dfrac{\partial w_3}{\partial\xi_0}\right) = -f_0'\dfrac{\partial}{\partial\xi_0}\left(\eta f_1'\dfrac{\partial w_2}{\partial\xi_1}\right)\\
\quad - f_1'\dfrac{\partial}{\partial\xi_1}\left(\eta f_0'\dfrac{\partial w_2}{\partial\xi_0}\right) - f_0'\dfrac{\partial}{\partial\xi_0}\left(\eta f_2'\dfrac{\partial w_1}{\partial\xi_2}\right)\\
\quad - f_1'\dfrac{\partial}{\partial\xi_1}\left(\eta f_1'\dfrac{\partial w_1}{\partial\xi_1}\right) - f_2'\dfrac{\partial}{\partial\xi_2}\left(\eta f_0'\dfrac{\partial w_1}{\partial\xi_0}\right)\\
\quad - f_0'\dfrac{\partial}{\partial\xi_0}\left(\eta f_3'\dfrac{\partial w_0}{\partial\xi_3}\right) - f_1'\dfrac{\partial}{\partial\xi_1}\left(\eta f_2'\dfrac{\partial w_0}{\partial\xi_2}\right)\\
\quad - f_2'\dfrac{\partial}{\partial\xi_2}\left(\eta f_1'\dfrac{\partial w_0}{\partial\xi_1}\right) - f_3'\dfrac{\partial}{\partial\xi_3}\left(\eta f_0'\dfrac{\partial w_0}{\partial\xi_0}\right)\\
\quad - \mathtt{i}f_0'\dfrac{\partial}{\partial\xi_0}\left(Gf_0'\dfrac{\partial w_1}{\partial\xi_0}\right) - \mathtt{i}f_0'\dfrac{\partial}{\partial\xi_0}\left(Gf_1'\dfrac{\partial w_0}{\partial\xi_1}\right)\\
\quad - \mathtt{i}f_1'\dfrac{\partial}{\partial\xi_1}\left(Gf_0'\dfrac{\partial w_0}{\partial\xi_0}\right) - \mathtt{i}\rho w_1,\\
w_3|_{\xi=\xi_a} = w_{a3},\\
s_{a3} = G\left(f_0'\dfrac{\partial w_1}{\partial\xi_0} + f_1'\dfrac{\partial w_0}{\partial\xi_1}\right)\bigg|_{\xi=\xi_a}\\
\quad -\mathtt{i}\eta\left(f_0'\dfrac{\partial w_3}{\partial\xi_0} + f_1'\dfrac{\partial w_2}{\partial\xi_1} + f_2'\dfrac{\partial w_1}{\partial\xi_2} + f_3'\dfrac{\partial w_0}{\partial\xi_3}\right)\bigg|_{\xi=\xi_a},\\
\lim\limits_{\xi_0\longrightarrow\infty} w_3 = 0.
\end{cases} \tag{33}$$

By substituting w_0, w_1 and w_2 from (32) into the differential equation in (33), we find that

$$\begin{aligned}
w_3 = &-\int\left\{\frac{1}{\eta f_0'}\left(\kappa_{01}\eta f_1'g_2 + \mathtt{i}\kappa_{01}\int\{\eta f_1'g_2'\}\right.\right.\\
&\left.\left.-\mathtt{i}\kappa_{01}^3\int\left\{\frac{\eta(f_1')^2}{f_0'}g_{01}\right\} - \kappa_{01}\int\left\{\frac{\rho}{f_0'}g_{01}\right\}\right)\right\}B_0\\
&\left(\int\left\{\kappa_{01}\frac{G}{\eta f_0'}\left(f_0'g_{01}' + f_1'\right)\right\}\right)B_0\\
&-\int\left\{\frac{1}{\eta f_0'}\left(\mathtt{i}\kappa_{01}\eta f_1'g_{02}' + \mathtt{i}\kappa_{01}\int\{\eta f_1'g_{02}'\} + \mathtt{i}\kappa_{01}\eta f_2'g_{01}\right.\right.\\
&\left.\left.+\mathtt{i}\kappa_{01}\int\{\eta f_2'g_{01}'\} + 2\mathtt{i}\kappa_{01}\int\left\{\frac{\eta f_2'f_1'}{f_0'}\right\}\right)\right\}\frac{\partial B_0}{\partial\xi_2}\\
&-\int\left\{\frac{1}{\eta f_0'}\left(\eta f_1'g_{11} + \int\{\eta f_1'g_{11}'\} + \int\left\{\frac{\eta(f_1')^2}{f_0'}\right\}\right)\right\}\frac{\partial^2 B_1}{\partial\xi_1^2}\\
&-\mathtt{i}\int\left\{\frac{1}{\eta f_0'}\int\frac{\rho}{f_0'}\right\}B_1\\
&-\int\left\{\frac{f_1'}{f_0'}\right\}\frac{\partial B_2}{\partial\xi_1} - \int\left\{\frac{f_2'}{f_0'}\right\}\frac{\partial B_1}{\partial\xi_2}\\
&-\int\left\{\frac{f_3'}{f_0'}\right\}\frac{\partial B_0}{\partial\xi_3} + \int\left\{\frac{1}{\eta f_0'}\right\}A_3 + B_3,
\end{aligned}$$

where all terms but B_3 diverge as $\xi_0 \to \infty$ for the same reasons exposed for first term of expression (10). There are signs of similarity with the structure of w_2 in the previous case. It is immediately obvious that A_3 can be related to the terms with first-order integral coefficients, that is, those of $\partial B_2/\partial\xi_1$, $\partial B_1/\partial\xi_2$ and $\partial B_0/\partial\xi_3$. Also, substitution of g_{11} into the coefficient of $\partial^2 B_1/\partial\xi_1^2$ reveals that it is exactly the same as that of $\partial^2 B_0/\partial\xi_1^2$ of w_2 and, together with the term in B_1, the same differential equation is formed as for B_0 with respect to the same variable ξ_1. It only remains to be seen how the terms of B_0 and $\partial B_0/\partial\xi_2$ would cancel out in the limit. Regarding this, one option is that they cancel each other by establishing a proportionality relation between B_0 and $\partial B_0/\partial\xi_2$, and the other option is that they cancel separately. The first option leads to an inconsistency in which f_2 would not behave asymptotically as required by (24). On the other hand, for the second option, it can immediately be seen that if the B_0 term must be zero at least in the limit, it would imply a condition on f_1 and the parameters of the medium. However, such a condition restricts the material parameters in a very capricious way. So, in order to maintain the maximum possible generality, the alternative is to take f_1 as the solution of the equation resulting from equating the coefficient of B_0 to zero. In addition, the term of $\partial B_0/\partial\xi_2$ must also become zero, for which there are three possibilities: the first one is that the coefficient cancels out in the limit, the second one is that it cancels out identically, and the third one is that $\partial B_0/\partial\xi_2 = 0$. In fact, the first two possibilities are inconsistent with the conditions for f_1 and f_2 in (24), leaving the third one as the only possibility. With such considerations, we have

$$\frac{\partial^2 B_1}{\partial\xi_1^2} = -\kappa_{11}^2 B_1, \tag{34}$$

$$A_3 = \alpha_{21}\frac{\partial B_2}{\partial\xi_1} + \alpha_{12}\frac{\partial B_1}{\partial\xi_2} + \alpha_{03}\frac{\partial B_0}{\partial\xi_3}, \tag{35}$$

$$\begin{aligned}&\int\left\{\frac{1}{\eta f_0'}\left(\kappa_{01}\eta f_1' g_2 + \mathtt{i}\kappa_{01}\int \eta f_1' g_2'\right.\right.\\ &\left.\left.-\mathtt{i}\kappa_{01}^3\int\frac{\eta(f_1')^2}{f_0'}g_{01} - \kappa_{01}\int\frac{\rho}{f_0'}g_{01}\right)\right\}\\ &-\int\left\{\kappa_{01}\frac{G}{\eta f_0'}\left(f_0' g_{01}' + f_1'\right)\right\} = 0,\end{aligned} \tag{36}$$

$$\frac{\partial B_0}{\partial\xi_2} = 0. \tag{37}$$

Now, define

$$\begin{aligned}g_3 = &\int\left\{\frac{1}{\eta f_0'}\left(\eta f_1' g_{11} + \int \eta f_1' g_{11}' + \int\frac{\eta(f_1')^2}{f_0'}\right)\right\}\kappa_{11}^2\\ &-\mathtt{i}\int\left\{\frac{1}{\eta f_0'}\int\frac{\rho}{f_0'}\right\},\end{aligned}$$

$$\begin{aligned}g_{21} &= \alpha_{21}\int\left\{\frac{1}{\eta f_0'}\right\} - \int\left\{\frac{f_1'}{f_0'}\right\},\\ g_{12} &= \alpha_{12}\int\left\{\frac{1}{\eta f_0'}\right\} - \int\left\{\frac{f_2'}{f_0'}\right\},\\ g_{03} &= \alpha_{03}\int\left\{\frac{1}{\eta f_0'}\right\} - \int\left\{\frac{f_3'}{f_0'}\right\},\end{aligned} \tag{38}$$

so $g_3 = g_2$ and $g_{21} = g_{11} = g_{01}$ for $\alpha_{21} = \alpha_{11} = \alpha_{01}$, and $g_{12} = g_{02}$ for $\alpha_{12} = \alpha_{02}$. Then, we write $w_3 = g_3 B_1 + g_{21}\partial B_2/\partial\xi_1 + g_{12}\partial B_1/\partial\xi_2 + g_{03}\partial B_0/\partial\xi_3 + B_3$. The wave equation of B_1 with respect to ξ_1 results in $\kappa_{11} = \kappa_{01}$. At this point we can already observe the recursiveness in the decision-making of the integration constant A_n and the dependence of each contribution w_n with respect to ξ_1. From this, it could even be deduced that most likely no other contribution w_n depends on ξ_2, something that in any case remains to be proven elsewhere. On the other hand, we have finally arrived at the equation that defines f_1: manipulating (36), it can be rewritten as

$$\begin{aligned}&\left(-\frac{\varsigma}{6}\right)\left(\frac{f_1}{\alpha_{01}}\right)^3 + \left(\frac{\varsigma}{2}\int\left\{\frac{1}{\eta}\right\}\right)\left(\frac{f_1}{\alpha_{01}}\right)^2\\ &\quad+\left(-\int\left\{\frac{1}{\eta}\int\rho\right\}\right)\left(\frac{f_1}{\alpha_{01}}\right)\\ &\quad+\left(\int\left\{\frac{1}{\eta}\int\left\{\rho\int\frac{1}{\eta}\right\}\right\} + \int\left\{\frac{G}{\eta^2}\right\}\right) = 0,\end{aligned} \tag{39}$$

where $\varsigma = -\mathtt{i}\alpha_{01}^2\kappa_{01}^2$. This cubic equation has analytical solutions given by [48]

$$\left(\frac{f_1}{\alpha_{01}}\right)_n = -\frac{1}{3a}\left(b + \left(\sqrt[3]{\mathtt{i}}\right)^n C_\pm + \frac{\Delta_0}{\left(\sqrt[3]{\mathtt{i}}\right)^n C_\pm}\right), \tag{40}$$

with $n \in \{0,1,2\}$, where $\Delta_0 = b^2 - 3ac$, $\Delta_1 = 2b^3 - 9abc + 27a^2 d$ and $C_\pm = \sqrt[3]{(\Delta_1 \pm \sqrt{\Delta_1^2 - 4\Delta_0^3})/2}$, being a, b, c, d the coefficients of the powers of f_1/α_{01} in equation (39) and $\sqrt[3]{\mathtt{i}} = (-1 + \mathtt{i}\sqrt{3})/2$.

It is necessary to verify that f_1/α_{01} satisfies condition (17). For this, rewrite Δ_0 and Δ_1 as

$$\begin{aligned}\Delta_0 &= \left(\frac{\varsigma}{2}\int\left\{\frac{1}{\eta}\right\}\right)^2\left(1 - \frac{\delta_1}{\varsigma}\right),\\ \Delta_1 &= \left(\frac{\varsigma}{2}\int\left\{\frac{1}{\eta}\right\}\right)^3\left(2 - 3\frac{\delta_1}{\varsigma} + \frac{\delta_2}{\varsigma}\right),\end{aligned}$$

where

$$\begin{aligned}\delta_1(\xi_0) &= \frac{\int\left\{\frac{1}{\eta}\int\rho\right\}}{\int\left\{\frac{1}{\eta}\int\frac{1}{\eta}\right\}},\\ \delta_2(\xi_0) &= \frac{\int\left\{\frac{1}{\eta}\int\left\{\rho\int\frac{1}{\eta}\right\}\right\} + \int\left\{\frac{G}{\eta^2}\right\}}{\int\left\{\frac{1}{\eta}\int\left\{\frac{1}{\eta}\int\frac{1}{\eta}\right\}\right\}},\end{aligned} \tag{41}$$

considering relations $\left(\int\{1/\eta\}\right)^2 = 2\int\{1/\eta\int\{1/\eta\}\}$ and $\left(\int\{1/\eta\}\right)^3 = 6\int\{1/\eta\int\{1/\eta\int\{1/\eta\}\}\}$ that can be verify directly. It follows that

$$C_\pm = \frac{\varsigma}{2}\int\left\{\frac{1}{\eta}\right\}\delta_3^\pm,$$

with

$$\delta_3^\pm(\xi_0) = \left(\left(2 - 3\frac{\delta_1}{\varsigma} + \frac{\delta_2}{\varsigma}\right)\right. \left.\pm\sqrt{\left(2-3\frac{\delta_1}{\varsigma}+\frac{\delta_2}{\varsigma}\right)^2 - 4\left(1-\frac{\delta_1}{\varsigma}\right)^3}\right)^{1/3}, \quad (42)$$

which, by substitution into (40), produces

$$\left(\frac{f_1}{\alpha_{01}}\right)_n = \int\left\{\frac{1}{\eta}\right\}\left(1+(\sqrt[3]{\mathtt{i}})^n\delta_3^\pm+\frac{1-\frac{\delta_1}{\varsigma}}{(\sqrt[3]{\mathtt{i}})^n\delta_3^\pm}\right), \quad (43)$$

with $n \in \{0,1,2\}$. Provided that δ_1 and δ_2 are finite for $\xi_0 \to \infty$, then $(f_1/\alpha_{01})_n$ would behave as desired, that is, they would be $\mathcal{O}\left(\int 1/\eta\right)$. Earlier we discussed the finitude of δ_1 in terms of the consistency of κ_{01}, but now it is necessary to assume that δ_2 is also finite, which seems sensible under the same arguments that the orders of integration of the parameters in the numerator and denominator are equal. That is, the obtained form of f_1/α_{01} is consistent with the requirement of its asymptotic behavior. Note that α_{01} serves as an indeterminate parameter, generally complex, whose determination from the data will be addressed in the validation section 5..

Now, we refocus on the objective of obtaining effective parameters. From (23) and (19), the homogenized problem is stated as

$$\begin{cases} \dfrac{\partial^2 B_0}{\partial\xi_1^2} + \kappa_{01}^2 B_0 = 0, \\ B_0|_{\xi=\xi_a} = w_{a0}, \\ s_{a1} = -\mathtt{i}\alpha_{01}\left.\dfrac{\partial B_0}{\partial\xi_1}\right|_{\xi=\xi_a}, \\ \lim\limits_{\xi_0\longrightarrow\infty} w_0 = 0, \end{cases} \quad (44)$$

where κ_{01} is the effective wave number, specific for this first approximate description version of the original problem in terms of the variable ξ_1. Apparently, there are three conditions, but it must be taken into account that response s_{a1} is considered unknown. The solution to problem (44) is

$$w_0(\xi_1) = w_{a0}\exp(\mathtt{i}\kappa_{01}\xi_1),$$
$$\alpha_{01}^2\kappa_{01}^2 = \mathtt{i}\lim_{\xi_0\to\infty}\frac{\int\left\{\frac{1}{\eta}\int\rho\right\}}{\int\left\{\frac{1}{\eta}\int\frac{1}{\eta}\right\}}, \quad (45)$$
$$s_{a1} = \alpha_{01}\kappa_{01}w_{a0}$$

with $\eta_a = \eta(\xi_0)|_{\xi=\xi_a}$. Referring to C_0 in (32) and the fact that B_0 does not depend on ξ_2, it was used that $C_0(\xi_3\ldots) \approx w_{a0}$ when $\ldots\xi_4 \ll \xi_3 \ll \xi_1$ due to boundary conditions. Recall that s_{an} depends on w_{an} due to the attenuation condition. From the physical point of view, we would say that the displacement w is the variable given or imposed as excitation to the system, whereas the strain $\partial_\xi w$ is the response variable, and $\xi = \xi_a$ is simultaneously the point of both application of the excitation and collection of the response.

The behavior of the contribution w_0 is obtained with $\xi_1 = \nu f_1(\xi_0)$. Since f_1 is not a linear function of ξ_0, the behavior of w_0 as a function of the variable ξ_0 is not necessarily simply harmonic. Since the shape of w_0 is not harmonic and it is not an explicit function of the original spatial variable ξ_0, κ_{01} is not the effective complex wave number as we need. In an effort to find a definition of such an effective parameter, the reasoning is as follows. If it is admitted that the limit

$$\langle\eta^{-1}\rangle = \lim_{\xi_0\to\infty}\frac{1}{\xi_0-\xi_a}\int_{\xi_a}^{\xi_0}\frac{1}{\eta(\mu)}d\mu, \quad (46)$$

exists, which defines the average of the reciprocal of the viscosity, in turn it is possible to define a local wave number

$$\kappa_{\text{loc}}(x) = l^{-1}\kappa_{01}\nu f_1'(x/l), \quad (47)$$

recalling that $\xi_0 = x/l$ and that x is the original space variable, in such a way that the average

$$\kappa_{\text{cum}}(x) = \frac{1}{x-a}\int_a^x \kappa_{loc}(\mu)d\mu, \quad (48)$$

has a well-defined limit when $x \to \infty$ as a result of (46) and (17). This average is obtained naturally from multiplying and dividing the exponential argument in (45) by $x-a$, then associating $\kappa_{01}\xi_1/(x-a)$ to resemble the wave number of a harmonic behavior.

In other words, the lowest-order non-zero solution (45) takes the form

$$w_0 = w_{a0}\exp(\mathtt{i}\kappa_{\text{cum}}(x)(x-a)). \quad (49)$$

At the same time, as it is needed that effective wave number be a constant that enclosed the global behavior of the layered medium, global average of κ_{loc} just lets us induce a definition of effective wave number as:

$$\kappa_{\text{eff}} = \lim_{x\to\infty}\kappa_{\text{cum}}(x) = \lim_{x\to\infty}\frac{1}{x-a}\int_a^x\kappa_{\text{loc}}(\mu)d\mu. \quad (50)$$

Substituting (47) into (50) and calculating the integral taking into account that $f_1(a/l) = 0$, we have that

$$\kappa_{eff} = \lim_{x\to\infty}\frac{\kappa_{01}\nu f_1(x/l)}{x-a},$$

which requires that, for the limit to exist, the asymptotic behavior of f_1 at infinity must be linear in x. It is known from Eq. (43) that the asymptotic behavior at infinity of f_1

is $\int \eta^{-1}$, provided that δ_1 and δ_2 are finite, as already mentioned. To guarantee this, it is sufficient that the functions G, η, and ρ be bounded throughout their domain; that is, that there exists an upper bound for the values of each of them. For example, if H_1 is a constant such that $|\eta^{-1}(\xi_0)| \leq H_1$ for all $\xi_0 \in [a/l, \infty)$, then $\int \eta^{-1} \leq H_1(\xi_0 - \xi_a) \sim H_1\xi_0$. Following a similar line of reasoning, one could arrive at $\int \left\{\eta^{-1} \int \eta^{-1}\right\} \leq H_2\xi_0^2$ and so on if more integrals are nested. The same applies to the G and ρ, resulting in similar inequalities for nested integrations of their combinations as well. Thus, in the case of δ_1 in Eq. (41), the numerator would be ξ_0^2 as well as the denominator, whereas in the case of δ_2, the numerator and denominator would be cubic powers. Requiring that the physical properties of shear modulus G, viscosity η, and mass density ρ be bounded is a natural and prudent requirement in this case. Thus, f_1 would be expected to behave asymptotically as $\xi_0 = x/l$ ensuring that the limit of κ_{eff} exists.

It is now convenient to express effective wave number as a function of the frequency ω for later use. To this end, we use (17) and (46) in (50) to get

$$\kappa_{\text{eff}} = l^{-1}\nu\langle\eta^{-1}\rangle\sqrt{\mathtt{i}\varsigma},$$

from which, by substituting $l^{-1} = \omega\sqrt{\tilde{\rho}/\tilde{G}}$ and $\nu = \sqrt{\tilde{G}}/\sqrt{\omega\tilde{\eta}}$, we get

$$\kappa_{\text{eff}} = \sqrt{\frac{\omega\tilde{\rho}}{\tilde{\eta}}}\langle\eta^{-1}\rangle\sqrt{\mathtt{i}\varsigma}, \tag{51}$$

which is the sought dependency because neither $\langle\eta^{-1}\rangle$ nor $\varsigma = -\mathtt{i}\alpha_{01}^2\kappa_{01}^2$ depend on ω. Parameter α_{01} has been associated with f_1 to obtain the average value of $1/\eta$. Once the effective complex wave number is obtained, propagation speed and attenuation are immediate to find because by writing the body of the harmonic wave as $e^{\mathtt{i}((\kappa_R+\mathtt{i}\kappa_I)x-\omega t)}$, where $\kappa_{\text{eff}} = \kappa_R + \mathtt{i}\kappa_I$, we have

$$\kappa_R = \frac{\omega}{v_{\text{eff}}}, \tag{52}$$

$$\kappa_I = \alpha_{\text{eff}}, \tag{53}$$

with v_{eff} the effective propagation speed and α_{eff} the effective attenuation.

Notably, this is to say that negative imaginary part $-\kappa_I$ becomes Floquet-Bloch's exponent when G, η and ρ are periodic functions [49,50]. Floquet-Bloch theory tells us that a solution of a differential equation like Eq. (5) with periodic coefficients sharing same period can be written as $e^{-kx}\psi(x)$ where ψ is a periodic function with period equal to that of the coefficients, e^{-kx} is the Floquet-Bloch factor and $-k$ is the Floquet-Bloch exponent or index. To see that $-\kappa_I$ is a Floquet-Bloch exponent we take solution (45) to its limit form when $\xi_0 \to \infty$. From Eq. (43), f_1 is dominated by the behavior of $\int \eta^{-1}$ in such a limit. Since η is periodic, say b-periodic, it is possible to write $\int \eta^{-1} = m_\eta(\xi_0 - \xi_a) + p_\eta(\xi_0)$ with $m_\eta = b^{-1}\int_{\xi_a}^{\xi_a+b} n^{-1}$ the mean value of η^{-1} over a period and $p_\eta(\xi_0)$ a suitable b-periodic function. Note that this linear growth is consistent with requirement of being η^{-1} bounded. Then, after some rearrangement, solution (45) is

$$\begin{aligned}
&\exp\left(\mathtt{i}\kappa_{01}\xi_1\right) = \exp\left(\mathtt{i}\sqrt{\mathtt{i}\varsigma}\nu\frac{f_1(\xi_0)}{\alpha_{01}}\right) \xrightarrow[\xi_0\to\infty]{} \\
&\exp\left(-\sqrt{\frac{\varsigma}{2}}\nu m_\eta(\xi_0-\xi_a)\right)\exp\left(-\sqrt{\frac{\varsigma}{2}}\nu p_\eta(\xi_0)\right)\times \\
&\exp\left(\mathtt{i}\sqrt{\frac{\varsigma}{2}}\nu\left(m_\eta(\xi_0-\xi_a)+p_\eta(\xi_0)\right)\right),
\end{aligned} \tag{54}$$

from which it is clear that as the last two exponential functions enclose exclusively periodic contributions, the first exponential function coincides with Floquet-Bloch factor and, therefore, $k = \sqrt{(\varsigma/2)}\nu m_\eta l^{-1}$ is the negative Floquet-Bloch exponent. Moreover, when η is periodic, it follows that $\langle\eta^{-1}\rangle = m_\eta$ and $\kappa_I = k$, so effective wave number definition is in accordance with what is expected from Floquet-Bloch theory. This shows that the results for periodic properties are recovered as a special case since no prior restriction has been assumed regarding the arrangement of the layers, which can even be arranged randomly.

The approximate solution u of the original problem (1) is found from the real part of (49). Section 5. presents some numerical solutions.

5. Validation

Now problem (3) will be solved numerically with the transfer matrix method [51,52], and compared with approximate solution (49).

Restricting problem (3) to each layer of the medium (see Fig. 1) we get

$$\begin{cases}
\dfrac{d^2\hat{w}_n}{dx^2} + \kappa_n^2\hat{w}_n(x) = 0, \quad x \in [x_n, x_{n+1}], \\
\hat{w}_n(x)\big|_{x=x_n} = \hat{w}_{n+1}(x)\big|_{x=x_n}, \\
G_n^*\dfrac{d\hat{w}_n}{dx}\Big|_{x=x_n} = G_{n+1}^*\dfrac{d\hat{w}_{n+1}}{dx}\Big|_{x=x_n},
\end{cases} \tag{55}$$

with $n = 1, \ldots, N$; $\hat{w}_n$ is the complex displacement field solution in the n-th layer, and $\kappa_n = \sqrt{\omega^2\hat{\rho}_n/G_n^*}$ with $\hat{\rho}_n$ and G_n^* the constant approximations of $\hat{\rho}(x)$ and $G^*(x,\omega)$ in the n-th layer. Note that $\hat{w}_n$ is not the n-th approximation order contribution w_n in the asymthotic expansion (6). In addition, the boundary and attenuation conditions are

$$\begin{cases}
\hat{w}_1(x)\big|_{x=x_0} = \hat{w}_0, \\
G_1^*\dfrac{d\hat{w}_1}{dx}\Big|_{x=x_0} = \hat{s}_0, \\
\lim\limits_{x\to\infty}\hat{w}_{N+1}(x) = 0,
\end{cases} \tag{56}$$

where $\hat{w}_0 = \hat{w}_a$ and $\hat{s}_0 = \hat{s}_a$ are the constant complex boundary values in $x = x_0 = a$.

The solution of problem (55) on the n-th layer is

$$\hat{w}_n(x) = A_n e^{\mathtt{i}\kappa_n x} + B_n e^{-\mathtt{i}\kappa_n x}, \tag{57}$$

where A_n and B_n are the integration constants. Taking into account that the stress in the n-th layer is $\hat{s}_n(x) = G_n^* d\hat{w}_n/dx$, we can write

$$\begin{bmatrix}\hat{w}_n(x)\\ \hat{s}_n(x)\end{bmatrix} = M_n(x)\begin{bmatrix}A_n\\ B_n\end{bmatrix}, \tag{58}$$

with

$$M_n(x) = \begin{bmatrix} e^{\mathtt{i}\kappa_n x} & e^{-\mathtt{i}\kappa_n x}\\ \mathtt{i}\kappa_n G_n^* e^{\mathtt{i}\kappa_n x} & -\mathtt{i}\kappa_n G_n^* e^{-\mathtt{i}\kappa_n x}\end{bmatrix}. \tag{59}$$

Since matrix $M_n(x)$ is non-singular, we have

$$\begin{bmatrix}A_n\\ B_n\end{bmatrix} = M_n^{-1}(x)\begin{bmatrix}\hat{w}_n(x)\\ \hat{s}_n(x)\end{bmatrix}, \tag{60}$$

where

$$M_n^{-1}(x) = \frac{1}{2\mathtt{i}\kappa_n G_n^*}\begin{bmatrix}\mathtt{i}\kappa_n G_n^* e^{-\mathtt{i}\kappa_n x} & e^{-\mathtt{i}\kappa_n x}\\ \mathtt{i}\kappa_n G_n^* e^{\mathtt{i}\kappa_n x} & -e^{\mathtt{i}\kappa_n x}\end{bmatrix}. \tag{61}$$

The continuity conditions in (55) can be written as

$$\begin{bmatrix}\hat{w}_{n+1}(x_n)\\ \hat{s}_{n+1}(x_n)\end{bmatrix} = \begin{bmatrix}\hat{w}_n(x_n)\\ \hat{s}_n(x_n)\end{bmatrix}, \quad n = 1, 2, \ldots, N, \tag{62}$$

from which it follows that

$$\begin{bmatrix}A_{n+1}\\ B_{n+1}\end{bmatrix} = M_{n+1}^{-1}(x_n) M_n(x_n)\begin{bmatrix}A_n\\ B_n\end{bmatrix}, \tag{63}$$

where (58) was used. This formula expresses the coefficients of the solution in the $(n+1)$-th layer as a function of those in the n-th. Then, the iterative application of formula (63) starting from $N+1$ produces

$$\begin{aligned}\begin{bmatrix}A_{N+1}\\ B_{N+1}\end{bmatrix} &= M_{N+1}^{-1}(x_N) M_N(x_N)\cdots M_{n+1}^{-1}(x_n)\\ &\times M_n(x_n) M_n^{-1}(x_{n-1}) M_{n-1}(x_{n-1})\cdots\\ &\times M_2^{-1}(x_1) M_1(x_1)\begin{bmatrix}A_1\\ B_1\end{bmatrix}.\end{aligned} \tag{64}$$

By left-multiplying (64) by matrix $M_{N+1}(x_N)$, then using (58) in $x = x_N$ to replace the product on the left-hand side, and using (60) to replace the column vector of layer $n = 1$ on the right-hand side, we obtain

$$\begin{aligned}\begin{bmatrix}\hat{w}_N\\ \hat{s}_N\end{bmatrix} &= M_N(x_N)\cdots M_{n+1}^{-1}(x_n) M_n(x_n) M_n^{-1}(x_{n-1})\\ &\times M_{n-1}(x_{n-1})\cdots M_1^{-1}(x_0)\begin{bmatrix}\hat{w}_0\\ \hat{s}_0\end{bmatrix},\end{aligned} \tag{65}$$

where $\hat{w}_N = \hat{w}_{N+1}(x_N) = \hat{w}_N(x_N)$ and $\hat{s}_N = \hat{s}_{N+1}(x_N) = \hat{s}_N(x_N)$. Define $T_n = M_n(x_n)M_n^{-1}(x_{n-1})$, so (65) can be rewritten as

$$\begin{bmatrix}\hat{w}_N\\ \hat{s}_N\end{bmatrix} = T\begin{bmatrix}\hat{w}_0\\ \hat{s}_0\end{bmatrix}, \tag{66}$$

where $T = T_N \cdots T_n \cdots T_1$, with

$$\begin{aligned} T_n &= M_n(x_n) M_n^{-1}(x_{n-1})\\ &= \begin{bmatrix}\cos(\kappa_n l_n) & \left(\frac{1}{\kappa_n G_n^*}\right)\sin(\kappa_n l_n)\\ -(\kappa_n G_n^*)\sin(\kappa_n l_n) & \cos(\kappa_n l_n)\end{bmatrix},\end{aligned} \tag{67}$$

and $l_n = x_n - x_{n-1}$ the thickness of the n-th layer, $n = 1, 2, \ldots, N$. The elementary case of (66) for a single layer allows observing that T_n connects the values at one end of the nth layer with the values at its other end, that is,

$$\begin{bmatrix}\hat{w}_n(x_n)\\ \hat{s}_n(x_n)\end{bmatrix} = T_n\begin{bmatrix}\hat{w}_n(x_{n-1})\\ \hat{s}_n(x_{n-1})\end{bmatrix}, \quad n = 1, 2, \ldots, N, \tag{68}$$

which means that if the values of displacement and stress on a boundary are known, then the corresponding values on the rest of the boundaries can be determined thanks to the continuity boundary conditions, and even the value at each point of the domain, as long as the parameters of each layer are known, namely, the thickness, the shear modulus of elasticity, the dynamical viscosity and the mass density. The first two boundary conditions of the relations (56) provide this information in principle, however, provided that the third of them is valid, which is the attenuation condition, one of the first two, displacement or stress, must remain unknown, that is, one of them would correspond to the imposed signal and the other to the response. In order to determine the response, it should be noted that the attenuation condition implies that the shape of the displacement in the $(N+1)$-th medium (x_N, ∞) is $\hat{w}_{N+1}(x) = A_{N+1}e^{\mathtt{i}\kappa_{N+1}x} + B_{N+1}e^{-\mathtt{i}\kappa_{N+1}x}$, where the first term corresponds to the plane wave traveling to the right [see Fig. 1b)], whereas the second term corresponds to a wave traveling to the left. Since the standing wave is imposed from the left on the $x = x_0$ boundary, it is expected to propagate to the right through each layer, generating transmission and reflection at each interface until reaching the $(N+1)$-th medium, where there would no longer be reflection but only propagation to the right. Hence, the coefficient of the leftward wave must be $B_{N+1} = 0$. From (60) we can see that $B_{N+1} = (\mathtt{i}\kappa_{N+1}G_{N+1}^* e^{\mathtt{i}\kappa_{N+1}x_N}\hat{w}_N - e^{\mathtt{i}\kappa_{N+1}x_N}\hat{s}_N)/(\mathtt{i}2\kappa_{N+1}G_{N+1}^*) = 0$, which implies that

$$\mathtt{i}\kappa_{N+1}G_{N+1}^*\hat{w}_N - \hat{s}_N = 0. \tag{69}$$

Note now that this new condition deduced from the wave attenuation condition requires knowledge of parameters κ_{N+1} and G_{N+1}^*. On the one hand, the wave is expected to be almost completely attenuated by the time it reaches the N+1st medium. This means that the contribution of these parameters is significantly reduced, but so is their inherent error, allowing for some freedom in their selection. In other words, the propagation involves only a few layers beyond which no information is available, so their parameters can be chosen conveniently. On the other hand, it is best if no further unknowns are introduced. Ideally, κ_{N+1} and G^*_{N+1} should be expressed in terms of the already known parameters of the other layers. One possibility is to use the same parameters as the last layer; another is to take the average parameters from the set of properties of the first few layers. The parameters used will be the equivalent parameters of the laminated medium. An equivalent medium is understood here as one whose parameters κ and G^* relate the displacements and stresses at the boundaries of the laminate through a relation similar to (68), that is,

$$\begin{bmatrix}\hat{w}_{N+1}\\ \hat{s}_{N+1}\end{bmatrix} = \begin{bmatrix}\cos(\kappa L) & \left(\frac{1}{\kappa G^*}\right)\sin(\kappa L)\\ -(\kappa G^*)\sin(\kappa L) & \cos(\kappa L)\end{bmatrix} \times \begin{bmatrix}\hat{w}_0\\ \hat{s}_0\end{bmatrix}, \tag{70}$$

where $L = l_1 + l_2 + \cdots + l_N = x_N - x_0$ is the total length of the composite medium. It should be noted that this idea of effectiveness is similar to the one proposed in Ref. [36] and explained as the black box idea in the introduction section. These parameters have been chosen because of their simple relationship with known parameters and because they encompass the entire laminated medium.

Equations (66), (69), (70) together with the imposed boundary condition, for example, $\hat{w}_0 = \text{const.}$, represent a system of six equations with six unknowns, namely, $\hat{w}_0$, $\hat{s}_0$, $\hat{w}_N$, $\hat{s}_N$, κ and G^*, but it must be kept in mind that $\kappa_{N+1} = \kappa$ y $G^*_{N+1} = G^*$, because of the construction of the effective medium.

It follows from (70) that

$$\cos(\kappa L) = \frac{\hat{w}_N\hat{s}_N + \hat{w}_0\hat{s}_0}{\hat{w}_N\hat{s}_0 + \hat{w}_0\hat{s}_N}, \tag{71}$$

$$(\kappa G^*)^2 = \frac{\hat{s}_0^2 - \hat{s}_N^2}{\hat{w}_N^2 - \hat{w}_0^2}. \tag{72}$$

Then, from (68), (69) and (72), we have

$$\left(r_{12}^2\right)(\mathtt{i}\kappa G^*)^4 + (2r_{11}r_{12})(\mathtt{i}\kappa G^*)^3 + \left(r_{11}^2 - r_{22}^2\right)(\mathtt{i}\kappa G^*)^2 + (-2r_{21}r_{22})(\mathtt{i}\kappa G^*) + \left(-r_{21}^2\right) = 0, \tag{73}$$

where r_{ij} are the components of matrix $R = T^{-1}$. Solving (73) for $\mathtt{i}\kappa G^*$, and then using (71) allows determining κ and G^*, which in turn reveals the relation between $\hat{w}_N$ and $\hat{s}_N$. With this relation, (69) and (66), it is possible to determine the two remaining unknowns having substituted the value imposed at the boundary. Regarding the four possible solutions of (73), only one has a consistent physical meaning.

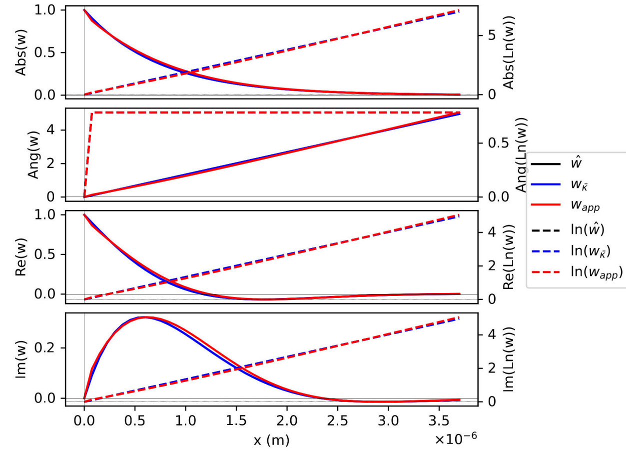

FIGURE 2. Comparison of solutions $\hat{w}$, $w_{\bar{\kappa}}$ and w_{app} for frecuency $\omega/2\pi = 10$ MHz and 1 layer. Vertical axes are dimensionless but the angle one is in rads. Right vertical axes in log scale apply for dashed lines.

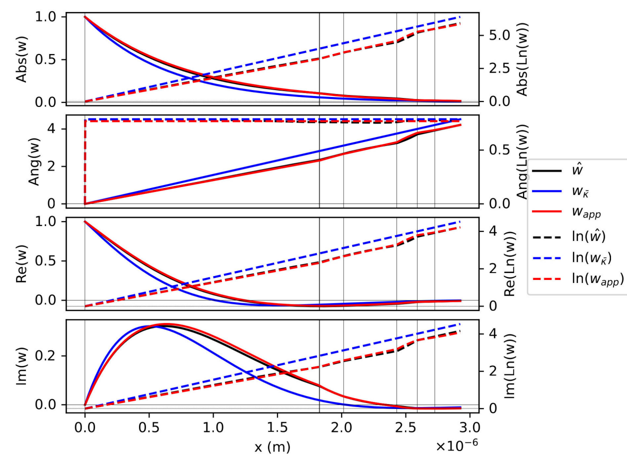

FIGURE 3. Same settings as in Fig. 2 but with 10 layers.

Figures 2-5 show the numerical solutions with the transfer matrix method denoted by $\hat{w}$ (black curves), the analytical solutions of lower order approximation (49) denoted by w_{app} (red curves) and, for comparison, the solutions when the parameter of the average complex wave number is used, weighted according to the width of the layers, denoted by $w_{\bar{\kappa}}$ (blue curves), obtained via the formulas

$$w_{\bar{\kappa}}(x) = w_a \exp(\mathtt{i}\bar{\kappa}(x - x_0)), \tag{74}$$

$$\bar{\kappa} = \frac{1}{L}\sum_{n=1}^{N} l_n \sqrt{\frac{\omega^2\hat{\rho}_n}{\hat{G}_n - \mathtt{i}\omega\hat{\eta}_n}}. \tag{75}$$

Vertical lines in gray indicate the interfaces, showing only those inside the attenuation range of the wave. In each figure, the top four subfigures show the real and imaginary parts of solutions $\hat{w}$, $w_{\bar{\kappa}}$ and w_{app}, as well as their absolute values and angles (left vertical axis and continuous curves), whereas the

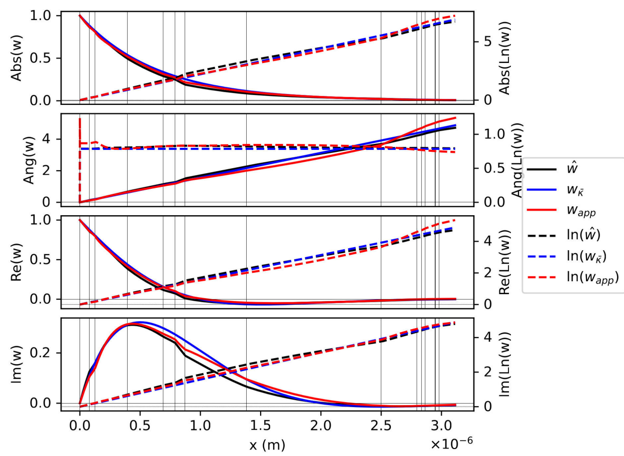

FIGURE 4. Same settings as in Fig. 2 but with 30 layers.

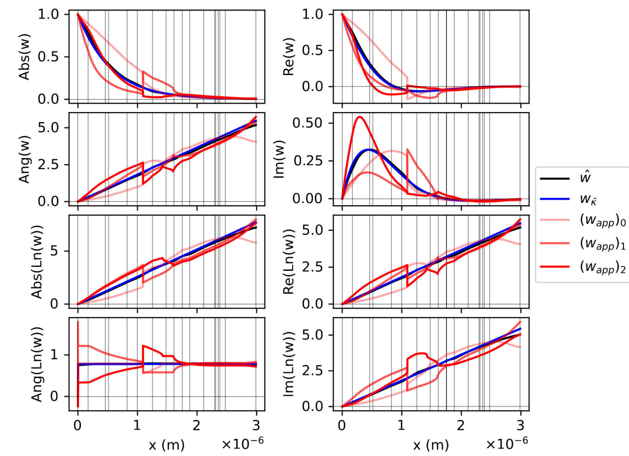

FIGURE 6. Comparison of solutions $\hat{w}$, $w_{\bar{\kappa}}$ and the three possible solutions for w_{app}. Frecuency $\omega/2\pi = 10$ MHz and 30 layers.

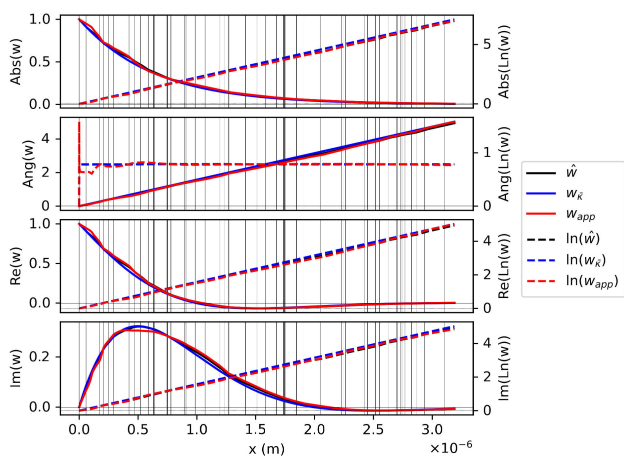

FIGURE 5. Same settings as in Fig. 2 but 100 layers.

right vertical axis is for natural logarithms of these quantities (dotted curves). Figures 2-5 correspond to 1, 10, 30 and 100 layers, respectively. The data sets of elasticity modulus, viscosity and density were generated randomly with standard distributions with average values from the data reported in Ref. [53] for bovine muscle tissue, therefore values $\tilde{G}$, $\tilde{\eta}$ and $\tilde{\rho}$ were taken as these average values as follows: $\tilde{G} = 0$, $\tilde{\eta} = 0.014$ Pa· s and $\tilde{\rho} = 1,080$ kg/m^3, and their standard deviations as $\sigma_G = 6,250$ Pa, $\sigma_\eta = 0.0035$ Pa·s and $\sigma_\rho = 0$, that is, constant density. The choice of these values comes from the fact that, around $G = 0$, the $\tilde{G}/\omega\tilde{\eta} \ll 1$ approximation is the best, on which the definition of the small expansion parameter is based. Frequency is set at $\omega = 10$ MHz, which is approximately where the curve of the elasticity modulus crosses the horizontal axis, that is, where it changes sign.

For soft tissue such as skeletal muscle, $\tilde{G}$ values close to zero and $\tilde{\eta} \sim 0.01$ Pa·s can be found according to [54] at frequencies ~ 15 MHz, whereas for hydrogel (a soft tissue substitute) the values are approximately $\tilde{G} \sim 100$ kPa and $\tilde{\eta} \sim 0.1$ Pa·s at frequencies ~ 100 MHz according to [55]. Unfortunately, the response of this type of material reported in literature at frequencies of MHz is scarce, largely because shear waves attenuate very quickly, as [53] points out, which makes the applicability of the results obtained here for these substitutes invalid, wich is why no graphics have been presented for these materials. On the other hand, an encouraging aspect is that the trend shown by [55] themselves for higher frequencies seems to indicate that the dominant viscosity regime would be reached for a frequency on the order of ~ 10 MHz fulfilling the assumption $\sqrt{\tilde{G}/\omega\tilde{\eta}} \ll 1$.

In general, at first glance, $w_{\bar{\kappa}}$ and w_{app} behave very similarly. However, tests with different groups of random data show that the w_{app} solution decreases in stability for increasing absolute value or dispersion of the elastic modulus data G and with increasing number of layers, which is expected in the first case, but not obvious in the second one. In fact, the greater the number of layers, the more frequently one can find behaviors like the one shown in Fig. 6, where jumps appear related to divisions by zero or changes of sign in the discriminant $\Delta_1^2 - 4\Delta_0^3$ associated with (39) in the numerical calculations. The yellow curves correspond to the different solution branches of w_{app} originating from the different solutions of f_1 (39). After testing with different data, we speculate that divisions by zero and sign changes of the discriminant seem to indicate opportunities to jump between the different solution branches, which could be tested in a future work. On the other hand, it should be noted that w_{app} seems to be effectively better than $w_{\bar{\kappa}}$ in those cases in which the distribution of layers is not uniform, which is better observed in the case of a low number of layers as in Fig. 3. Moreover, w_{app} accompanies the numerical solution $\hat{w}$ in its breaks or non-smooth changes at the interfaces, whereas $w_{\bar{\kappa}}$ does not due to its average nature. Also, the difference between the effective complex wave number (51) to (75) is less than 5%. Finally, it is important to take into account, from a methodological point of view, that the constant α_{01} was absorbed in the definition of f_1. This constant was optimally chosen to fit the numerical solution w, that is, to select the best approximate solution as the one with the best least-squares fit.

6. Conclusions

Seeking to build models for biomaterials, this work addressed the problem of shear-type waves emitted at the boundary of a laminated medium with layers made of homogeneous Voigt-type viscoelastic materials. The focus was placed on what happens in the immediate environment of the ray of incidence, with propagation perpendicular to the interfaces, so plane waves do not disperse in longitudinal waves or by changes of direction. The model was transformed into a perturbation problem and studied via the multiple scales method, from which the lowest nonzero order approximate solution was obtained with respect to the expansion parameter $\sqrt{\tilde{G}/\omega\tilde{\eta}} \ll 1$, which can be interpreted as the viscous relaxation being much smaller than the propagation period of the harmonic plane wave. The thermal effects derived from local friction were neglected, which means that the alterations in the parameters due to temperature changes caused by the mechanical propagation are not taken into account. The layers were taken to have random parameters close to the values for bovine muscle tissue reported in Ref. [53] in the frequency range of 10 MHz for which the elastic modulus G approaches zero and the viscosity is relatively constant.

The results obtained via the multiple scales method are applicable to situations where the excitation frequency is moderately high, so the effects of nonlinear responses can be neglected. It can be noted that the use of information from the medium and the excitation signal to define the appropriate expansion parameter is crucial, resulting in important simplifications of analysis.

Unlike classical homogenization (*e.g.*, [56]), this formulation is applicable to non-periodic structures. It allows for obtaining analytical expressions, in contrast to the numerical solution approach, and opens new avenues of connection with other problems. For example, the coefficients of the differential equation (G, η, and ρ) can be not only piecewise constant functions but also continuous, like a sinusoidal periodic function as in the Mathieu equation [57]. Furthermore, it focuses on the dependence of the material's response on the strain rate (frequency), making it clear that the interpretation of the constitutive parameters of the Voigt model must be done in terms of a frequency range.

Comparison was made to the results of the transfer matrix method, which is easily generalizable to any number of layers without making the expressions and computation more complex, with little loss of accuracy. Such expressions are useful for approximating the behavior of non-homogeneous media with piecewise continuous parameters, which allows the direct numerical treatment of the integrals. In fact, they are useful for media with random parameters of constant mean. Although further tests are needed in addition to numerical ones, such as dimensionless analysis, the variation with respect to the length fraction parameters l_n or others, as well as a more formal determination of the error, the results obtained so far are of practical value with relative low complexity.

Regarding the accuracy of the analytical expressions of lower order approximation (49) in comparison to the weighted wave number solution, it was observed that, in general, the former is not better than the latter. However, the lower order approximation solution has the virtue of reproducing the variations due to the structure of the medium, that is, to the value changes in the parameters of the propagation medium, which has the potential to transport information from the medium to the response signal and to decode it.

As future work, we can mention the application of these ideas to the design of agar-based phantoms with parameters guided via concentration, which would allow, from a theoretical point of view, the analysis of a greater number of configurations to evaluate their feasibility of implementation. In addition, the formulation will be generalized to more dimensions, considering the possibility of more elaborate geometries. In fact, these results would be part of a broader numerical simulation study, which in turn shortens the path for parameter estimation in situations of varying complexity. On the other hand, attenuation models in terms of conduction and internal friction could be incorporated to describe the dependence on the structure of the medium which, in turn, would lead to the proposal of possibly more appropriate constitutive models.

Acknowledgments

The authors would like to thank the SECIHTI (formerly CONAHCYT) postdoctoral fellowship program and the PAPIIT DGAPA UNAM IN102026 project, as well as the staff of the IIMAS host institute and journal reviewers for their comments.

---

1. R. W. Prager *et al.*, Three-dimensional ultrasound imaging, Proceedings of the Institution of Mechanical Engineers, Part H: Journal of Engineering in Medicine **224** (2010) 193-223, `https://doi.org/10.1243/09544119jeim586`

2. L. Mercier *et al.*, A review of calibration techniques for freehand 3-D ultrasound systems, Ultrasound in Medicine and Biology **31** (2005) 143-165, `https://doi.org/10.1016/j.ultrasmedbio.2004.11.001`

3. J. E. Aldrich, Basic physics of ultrasound imaging, Critical Care Medicine **35** (2007) S131-S137, `https://doi.org/10.1097/01.ccm.0000260624.99430.22`

4. A. Maccabi *et al*., Quantitative characterization of viscoelastic behavior in tissue-mimicking phantoms and ex vivo animal tissues, PLOS ONE **13** (2018) e0191919, `https://doi.org/10.1371/journal.pone.0191919`

5. M. H. Mozaffari and W.-S. Lee, Freehand 3-D Ultrasound

Imaging: A Systematic Review, Ultrasound in Medicine and Biology **43** (2017) 2099-2124, https://doi.org/10.1016/j.ultrasmedbio.2017.06.009

6. A. Fenster and D. B. Downey, Three-Dimensional Ultrasound Imaging, Annual Review of Biomedical Engineering **2** (2000) 457-475, https://doi.org/10.1146/annurev.bioeng.2.1.457

7. P.-W. Hsu *et al.*, Freehand 3D Ultrasound Calibration: A Review, p. 47-84 (Springer Berlin Heidelberg, 2008), https://dx.doi.org/10.1007/978-3-540-68993-5_3.

8. S. Wood *et al.,* Design and fabrication of a realistic anthropomorphic heterogeneous head phantom for MR purposes, PLOS ONE **12** (2017) e0183168, https://doi.org/10.1371/journal.pone.0183168

9. M. Earle, G. D. Portu, and E. DeVos, Agar ultrasound phantoms for low-cost training without refrigeration, African Journal of Emergency Medicine **6** (2016) 18-23, https://doi.org/10.1016/j.afjem.2015.09.003

10. S. Cournane, A. J. Fagan, and J. E. Browne, Review of ultrasound elastography quality control and training test phantoms, Ultrasound **20** (2011) 16-23, https://doi.org/10.1258/ult.2011.011033

11. J. Bravo-Castillero and L. F. López Ríos, Variational formulation for fractional hyperbolic problems in the theory of viscoelasticity, Zeitschrift für angewandte Mathematik und Physik **73** (2022), https://doi.org/10.1007/s00033-022-01826-5

12. K. Manickam, R. R. Machireddy, and S. Seshadri, Characterization of biomechanical properties of agar based tissue mimicking phantoms for ultrasound stiffness imaging techniques, Journal of the Mechanical Behavior of Biomedical Materials **35** (2014) 132-143, https://doi.org/10.1016/j.jmbbm.2014.03.017

13. T. A. Bigelow and W. D. O'Brien, Scatterer size estimation in pulse-echo ultrasound using focused sources: Calibration measurements and phantom experiments, *The Journal of the Acoustical Society of America* **116** (2004) 594-602, https://doi.org/10.1121/1.1757453

14. T. A. Bigelow and W. D. O'Brien, Scatterer size estimation in pulse-echo ultrasound using focused sources: Theoretical approximations and simulation analysis, *The Journal of the Acoustical Society of America* **116** (2004) 578-593, https://doi.org/10.1121/1.1757452

15. R. W. Gill, Physics and technology of diagnostic ultrasound: a practitioner's guide, 2nd ed. (High Frequency Publishing, S.l., 2020), p. 17-24.

16. K. Martin and K. Ramnarine, Physics, In P. R. Hoskins, K. Martin, and A. Thrush, eds., Diagnostic ultrasound: physics and equipment, 3rd ed., p. 7-36 (CRC Press, Boca Raton London New York, 2019), https://doi.org/10.1201/9781138893603

17. G. A. Holzapfel and R. W. Ogden, Modeling the biomechanical properties of soft biological tissues: Constitutive theories, *European Journal of Mechanics-A/Solids* **112** (2025) 105634, https://doi.org/10.1016/j.euromechsol.2025.105634

18. L. A. Taber, Nonlinear theory of elasticity: applications in biomechanics, 1st ed. (World Scientific, River Edge, NJ, 2004), pp. 247-264.

19. C. W. J. Oomens *et al.*, Biomechanics: concepts and computation, Cambridge texts in biomedical engineering, 2nd ed. (Cambridge University Press, Cambridge, United Kingdom; New York, NY, 2018), pp. 270-285.

20. S. Mohammadi, Multiscale biomechanics: theory and applications, 1st ed. (JohnWiley and Sons Ltd, Hoboken, NJ, 2023), pp. 23-74.

21. Y. C. Fung, Biomechanics: mechanical properties of living tissues, 2nd ed. (Springer-Verlag, New York, 1993), pp. 220-314.

22. A. Al-Mayah, ed., Biomechanics of soft tissues: principles and applications, 1st ed. (CRC Press, Boca Raton London New York, 2018), pp. 1-25.

23. V. Andreev, N. Tsybin, and R. Turusov, Layered composite and contact layer. Effective modulus of elasticity, *E3S Web of Conferences* **97** (2019) 04071, https://doi.org/10.1051/e3sconf/20199704071

24. J. Willis, Exact effective relations for dynamics of a laminated body, *Mechanics of Materials* **41** (2009) 385-393, https://doi.org/10.1016/j.mechmat.2009.01.010

25. J. Bravo-Castillero *et al.,* Homogenization of magneto-electroelastic multilaminated materials, *The Quarterly Journal of Mechanics and Applied Mathematics* **61** (2008) 311-332, https://doi.org/10.1093/qjmam/hbn010

26. M. S. Chaki and J. Bravo-Castillero, Dynamic asymptotic homogenization for wave propagation in magneto-electro-elastic laminated composite periodic structure, *Composite Structures* **322** (2023) 117410, https://doi.org/10.1016/j.compstruct.2023.117410

27. A. Srivastava and S. Nemat-Nasser, Overall dynamic properties of three-dimensional periodic elastic composites, Proceedings of the Royal Society A: Mathematical, *Physical and Engineering Sciences* **468** (2011) 269-287, https://doi.org/10.1098/rspa.2011.0440

28. J. H. McElhaney, Dynamic response of bone and muscle tissue, *Journal of Applied Physiology* **21** (1966) 1231, https://doi.org/10.1152/jappl.1966.21.4.1231

29. N. W. Tschoegl, The Phenomenological Theory of Linear Viscoelastic Behavior (Springer Berlin Heidelberg, 1989), pp. 35-145, https://dx.doi.org/10.1007/978-3-642-73602-5

30. N. Arnold, J. Scott, and T. R. Bush, A review of the characterizations of soft tissues used in human body modeling: Scope, limitations, and the path forward, *Journal of Tissue Viability* **32** (2023) 286-304, https://doi.org/10.1016/j.jtv.2023.02.003

31. S. J. Mostafavi Yazdi and J. Baqersad, Mechanical modeling and characterization of human skin: A review, *Journal of Biomechanics* **130** (2022) 110864, https://doi.org/10.1016/j.jbiomech.2021.110864

32. S. Catheline *et al.,* Measurement of viscoelastic properties of homogeneous soft solid using transient elastography: An inverse problem approach, *The Journal of the Acoustical Society of America* **116** (2004) 3734-3741, https://doi.org/10.1121/1.1815075

33. B. Zhou and X. Zhang, Comparison of five viscoelastic models for estimating viscoelastic parameters using ultrasound shear wave elastography, *Journal of the Mechanical Behavior of Biomedical Materials* **85** (2018) 109-116, https://doi.org/10.1016/j.jmbbm.2018.05.041
34. A. H. Nayfeh, Perturbation Methods (Wiley, 2000), p. 228-302, https://dx.doi.org/10.1002/9783527617609.
35. D. Cioranescu and P. Donato, An Introduction to Homogenization (Oxford University PressOxford, 1999), p. 125-133, https://dx.doi.org/10.1093/oso/9780198565543.001.0001
36. A. Srivastava and S. Nemat-Nasser, On the limit and applicability of dynamic homogenization, *Wave Motion* **51** (2014) 1045-1054, https://doi.org/10.1016/j.wavemoti.2014.04.003
37. R. M. Christensen, Mechanics of Composite Materials (Wiley, 1979), pp. 32-37, https://dx.doi.org/10.1115/1.3153710
38. N. Bakhvalov and G. Panasenko, Homogenisation: Averaging Processes in Periodic Media (Springer Netherlands, 1989), p. 12-29, https://dx.doi.org/10.1007/978-94-009-2247-1
39. R. M. Christensen, Theory of Viscoelasticity, An Introduction, 2nd Edition (ACADEMIC PRESS, 1982), p. 226-226, https://dx.doi.org/10.1115/1.3167591
40. R. M. Christensen, Theory of Viscoelasticity, An Introduction, 2nd Edition (ACADEMIC PRESS, 1982), p. 21-22, https://dx.doi.org/10.1115/1.3167591
41. M. Van Dyke and S. Rosenblat, Perturbation Method in Fluid Mechanics, *Journal of Applied Mechanics* **43** (1976) 189-190, https://doi.org/10.1115/1.3423785
42. A. Bensoussan*et al.*, Asymptotic Analysis of Periodic Structures, *Journal of Applied Mechanics* **46** (1979) 477-477, https://doi.org/10.1115/1.3424588
43. R. V. Craster, J. Kaplunov, and A. V. Pichugin, High-frequency homogenization for periodic media, Proceedings of the Royal Society A: Mathematical, *Physical and Engineering Sciences* **466** (2010) 2341-2362, https://doi.org/10.1098/rspa.2009.0612
44. C. M. Bender and S. A. Orszag, Advanced Mathematical Methods for Scientists and Engineers I (Springer New York, 1999), p. 560-567, https://doi.org/10.1007/978-1-4757-3069-2
45. C. M. Bender and L. M. A. Bettencourt, Multiple-scale analysis of quantum systems, *Physical Review D* **54** (1996) 7710-7723, https://doi.org/10.1103/physrevd.54.7710
46. M. J. Lighthill, A Technique for Rendering Approximate Solutions to Physical Problems Uniformly Convergent, *Philosophical Magazine* **40** (1949) 1179
47. J. Kevorkian and J. D. Cole, Multiple Scale and Singular Perturbation Methods (Springer New York, 1996), pp. 614- 617, https://dx.doi.org/10.1007/978-1-4612-3968-0
48. J. V. Uspensky, Theory of equations., McGraw-Hill paperbacks, 1st ed. (New York, 1948), pp. 93-107, OCLC: 525463.
49. M. S. P. M. S. P. Eastham, The spectral theory of periodic differential equations (Edinburgh, Scottish Academic Press [distributed by Chatto and Windus, London], 1973), pp. 1-5, https://archive.org/details/spectraltheoryof0000east
50. M. Humi and W. Miller, Second Course in Ordinary Differential Equations for Scientists and Engineers, Universitext (Springer US, New York, NY, 1988), pp. 215-221.
51. A. Dell, A. Krynkin, and K. Horoshenkov, The use of the transfer matrix method to predict the effective fluid properties of acoustical systems, *Applied Acoustics* **182** (2021) 108259, https://doi.org/10.1016/j.apacoust.2021.108259
52. T. G. Mackay and A. Lakhtakia, The Transfer-Matrix Method in Electromagnetics and Optics (Springer International Publishing, 2020), pp. 25-26, http://dx.doi.org/10.1007/978-3-031-02022-3
53. E. L. Madsen, H. J. Sathoff, and J. A. Zagzebski, Ultrasonic shear wave properties of soft tissues and tissuelike materials, *The Journal of the Acoustical Society of America* **74** (1983) 1346-1355, https://doi.org/10.1121/1.390158
54. Xinmai Yang and C. Church, A simple viscoelastic model for soft tissues the frequency range 6-20 MHz, IEEE Transactions on Ultrasonics, *Ferroelectrics and Frequency Control* **53** (2006) 1404, https://doi.org/10.1109/TUFFC.2006.1665097
55. X. Feng, G.-Y. Li, and S.-H. Yun, Ultra-wideband optical coherence elastography from acoustic to ultrasonic frequencies, *Nature Communications* **14** (2023) 4949, https://doi.org/10.1038/s41467-023-40625-y
56. J. Bravo-Castillero *et al.*, Mathematical Modelling of Composite Phantoms for the Calibration of Ultrasound Devices, *Journal of Applied Research and Technology* **21** (2023) 154, https://doi.org/10.22201/icat.24486736e.2023.21.2.1535
57. F. M. Arscott, Periodic Differential Equations: An Introduction to Mathieu, Lamé, and Allied Functions (Elsevier, 2014), pp. 26-29.